CONF-8310102--2

A WIDE-RANGE VORTEX SHEDDING FLOWMETER FOR HIGH-TEMPERATURE HELIUM GAS*

CONF-8310102--2

DE84 001984

S. P. Baker†
P. G. Herndon†
R. M. Ennis, Jr.**

ABSTRACT

The existing design of a commercially available vortex shedding flowmeter (VSFM) was modified and optimized to produce three 4-in. and one 6-in. high-performance VSFMs for measuring helium flow in a gas-cooled fast reactor (GCFR) test loop. The project was undertaken because of the significant economic and performance advantages to be realized by using a single flowmeter capable of covering the 166:1 flow range (at 350°C and 45:1 pressure range) of the tests. A detailed calibration in air and helium at the Colorado Engineering Experiment Station showed an accuracy of ±1% of reading for a 100:1 helium flow range and ±1.75% of reading for a 288:1 flow range in both helium and air. At an extended gas temperature of 450°C, water cooling was necessary for reliable flowmeter operation.

INTRODUCTION

A flowmeter was required for measuring recirculating helium gas flow over a wide range of conditions in a gas-cooled fast reactor (GCFR) test loop. The flow measurement requirements of the GCFR test loop exceeded the proven performance of any single conventional flowmeter. A special-purpose vortex shedding flowmeter (VSFM) was developed because a single flowmeter capable of meeting all GCFR test loop requirements would provide significant economic and performance advantages in the operation of the loop.

In this report the authors discuss the development, conceptual design, and final design of a modified VSFM. The results of extensive flow calibration of the flowmeter at the Colorado Engineering Experiment Station (CEES) are presented. Some operating experience with the flowmeters is discussed, both within the design envelope and at an extended gas temperature of 450°C. The report concludes with recommendations for application of this

undertaken because of the significant economic and performance advantages to be realized by using a single flowmeter capable of covering the 166:1 flow range (at 350°C and 45:1 pressure range) of the tests. A detailed calibration in air and helium at the Colorado Engineering Experiment Station showed an accuracy of ±1% of reading for a 100:1 helium flow range and ±1.75% of reading for a 288:1 flow range in both helium and air. At an extended gas temperature of 450°C, water cooling was necessary for reliable flowmeter operation.

INTRODUCTION

A flowmeter was required for measuring recirculating helium gas flow over a wide range of conditions in a gas-cooled fast reactor (GCFR) test loop. The flow measurement requirements of the GCFR test loop exceeded the proven performance of any single conventional flowmeter. A special-purpose vortex shedding flowmeter (VSFM) was developed because a single flowmeter capable of meeting all GCFR test loop requirements would provide significant economic and performance advantages in the operation of the loop.

In this report the authors discuss the development, conceptual design, and final design of a modified VSFM. The results of extensive flow calibration of the flowmeter at the Colorado Engineering Experiment Station (CEES) are presented. Some operating experience with the flowmeters is discussed, both within the design envelope and at an extended gas temperature of 450°C. The report concludes with recommendations for application of this VSFM to the GCFR test loop.

ENGINEERING CONSIDERATIONS

The GCFR test loop is a high-temperature, high-pressure helium gas circulating loop in which a bundle of rods is electrically heated to simulate portions of the fuel and control rod elements of a full-size blanket element of a GCFR core (Figure 1 is a flow diagram of the GCFR test loop). The test bundle is subjected to controlled electric power and helium gas flow conditions that simulate the GCFR operating conditions anticipated during steady-state operation, normal upsets, and emergency and depressurization transients. The experimental results from these tests will be applied to verify the analytical methods used to design the GCFR core elements and to determine whether the elements will withstand the anticipated conditions.

---

*Research sponsored by the Office of Converter Reactor Deployment, U.S. Department of Energy under contract W-7405-eng-26 with the Union Carbide Corporation.

†Oak Ridge National Laboratory, Instrumentation and Controls Division, P.O. Box X, Oak Ridge, TN 37830.

**American Magnetics, Inc., 112 Flint Road, Oak Ridge, TN 37830

DISCLAIMER

The operating requirements for a flowmeter for this application include: (1) a volumetric flow accuracy of ±1.0% of reading over a Pipe Reynolds Number (R_D) range from 6×10^3 to 1×10^6 at pressures from 0.2 to 9 MPa (29 to 1305 psia) and at 350°C in 4-in. and 6-in. schedule 80 pipe, (2) a fast response time (<0.1 s), (3) a maintained accuracy during flow and pressure transients, and (4) a low pressure drop across the flowmeter. Also, to maintain the helium gas at a high level of purity, the flowmeter must not be a source of contaminants.

From a survey and studies to find a suitable flowmeter for this application, we chose a commercial VSFM design, Eastech Model 2500. The design selected has a thermal sensor remotely located from the flowing gas. However, no performance data for it were available under conditions similar to this application, and, furthermore, this design was unavailable commercially in meter sizes smaller than 8 in.

To determine the performance characteristics of this design (its rangeability and accuracy) for high-temperature helium flow measurement, several unassembled commercial VSFM components [flow element (bluff body), thermal sensor, and signal processor] were obtained from the manufacturer(1) for assembly into a 4-in. meter. To achieve wide rangeability, we optimized the design and size of the flowmeter to be compatible with the GCFR test loop.

SUMMARY OF DEVELOPMENT WORK(2, 3)

To obtain the required rangeability for this application, a flowmeter design employing a thermal sensor remotely located from the high temperature gas was chosen. The relationships of sensor signal, remote connecting tubing geometry, and flow conditions were investigated in an open-loop system in order to determine and optimize the sensitivity of this design. The minimum sensor signal required to produce a reliable output from the associated signal conditioner was also determined.

Design Approach

Two characteristics determine the rangeability of a VSFM in a given application, namely, the range of linearity of the meter, and the sensitivity of the meter over the required range of flowing conditions, where sensitivity is the peak-to-peak thermal sensor output for a given gas density and volumetric flow rate. The inherent nominal linearity(4) of a VSFM can be 0.5-1.0% of its reading in an R_D range from 10^4 to $>10^6$. In this application the primary problem in achieving wide rangeability is in attaining adequate sensitivity over this R_D range at all densities, particularly at low density, low flow conditions.

Although both electromechanical and thermal sensors were available, a thermal sensor (a self-heated thermistor) was chosen as the vortex shedding sensor because it has higher sensitivity than electromechanical types over the wide range of flow conditions in this application. A thermal sensor was selected because it has a high signal-to-noise ratio and a good frequency response. However, because its maximum operating temperature limit is nominally 200°C, the thermal sensor is installed at a location remote from the high

relationships of sensor signal, remote connecting tubing geometry, and flow conditions were investigated in an open-loop system in order to determine and optimize the sensitivity of this design. The minimum sensor signal required to produce a reliable output from the associated signal conditioner was also determined.

Design Approach

Two characteristics determine the rangeability of a VSFM in a given application, namely, the range of linearity of the meter, and the sensitivity of the meter over the required range of flowing conditions, where sensitivity is the peak-to-peak thermal sensor output for a given gas density and volumetric flow rate. The inherent nominal linearity(4) of a VSFM can be 0.5-1.0% of its reading in an R_D range from 10^4 to $>10^6$. In this application the primary problem in achieving wide rangeability is in attaining adequate sensitivity over this R_D range at all densities, particularly at low density, low flow conditions.

Although both electromechanical and thermal sensors were available, a thermal sensor (a self-heated thermistor) was chosen as the vortex shedding sensor because it has higher sensitivity than electromechanical types over the wide range of flow conditions in this application. A thermal sensor was selected because it has a high signal-to-noise ratio and a good frequency response. However, because its maximum operating temperature limit is nominally 200°C, the thermal sensor is installed at a location remote from the high-temperature gas flow; the gas is routed by pressure taps to a lower ambient temperature region (Fig. 2).

The assembly consists of a bluff body, connecting tubing that extends from each side of the bluff body to a remote sensor block, a thermal sensor assembly, and a signal conditioner. The bluff body is permanently mounted and aligned in the meter body, using precision dowels. Connecting tubing transmits to the sensor the pressure pulse associated with each shed vortex. The sensor block has shutoff valves to permit removal of the sensor without opening the flow system to atmospheric pressure. The path from the bluff body through the connecting tubing, valves, and sensor block is designed for minimum flow noise.

The sensor assembly detects changes in the gas velocity that result from pressure pulses produced by shed vortices. The signal conditioner includes a constant current source and a circuit that converts the millivolt-level, sinusoidal sensor output to a 5-V peak-to-peak (p-p), square-wave signal.

The entire assembly (including meter body, mounting block, and tubing) is stainless steel. Since there is negligible net gas flow through the tubing loop from one side of the bluff body to the other, heat transfer from the metered gas flow to the remote sensor is limited to conduction through the tubing and radiation from the pipe wall, which is covered with 2 in. of Kaowool insulation.

Sensitivity Considerations

In the remote sensor design, three factors determine sensitivity, namely:

- Amplitude of vortex-generated pressure pulses as a function of flowing conditions,
- Thermal response curve of the sensor assembly,
- Pressure pulse attenuation in the connecting tubing.

The variation of the amplitude of vortex-generated pressure pulses with flowing conditions is complex. To a first approximation, the amplitude is proportional to ρq^2, where ρ is the density and q is the volumetric flow rate.(5)

The thermal response of the sensor assembly depends on the temperature, the geometry, and the specific heat capacity of the self-heated thermistor, and on the film coefficient of the gas at the sensor surface.(6) The thermal respoonse of the sensor assembly over the entire flow range would be difficult to analytically predict satisfactorily.

The variation of pressure pulse attenuation in the connecting tubing over the range of flowing conditions was unknown.

These factors were investigated experimentally to learn more about them and to determine their interrelated effects on meter sensitivity.

Signal Conditioner Threshold Response

To determine the minimum sensor signal required to produce a reliable square-wave output, the threshold response of the signal conditioner was measured over the vortex shedding frequency range (0-400 Hz). The threshold response is defined as the minimum peak-to-peak input voltage that will reliably trigger a square-wave output.

The results of these response tests are plotted in Figure 3. The applied voltage V_a across the sensor was optimized for the impedance of the sensor to produce a minimum threshold. A 60-Hz noise level of 300 µV was observed over the entire frequency range, which we attribute to the ripple from the VSFM constant current source.

Based on the results shown in Figure 3, we concluded that the nominal input threshold of the signal conditioner is 1.0 mV p-p, which represents a nominal signal-to-noise ratio of 3:1. Therefore, to produce a reliable output from the signal conditioner over the entire input frequency range, a minimum sensor signal of 1.0 mV p-p must be maintained for all flow conditions.

Flow Testing of Remote Sensor Design

Measurements were made over a wide range of flow, density, and temperature conditions to establish the empirical relationships of sensor signal, connecting tubing geometry, and flow conditions so that we could optimize the sensitivity. The following relationships were investigated:

- Variation of the vortex signal as a function of flow conditions,
- Attenuation of the vortex signal as a function of the connecting tubing geometry,
- Ratio of sensor signal-to-noise as a function of the connecting tube geometry and flow conditions,
- Increase of the remote sensor temperature above ambient due to flow conditions.

Remote Sensor Signal Performance

All measurements were made using the ORNL-assembled 4-in. VSFM. Both the sensor signal and the square-wave output of the signal conditioner were observed simultaneously on a dual-channel storage oscilloscope. Oscilloscope traces for low flow and high flow conditions are shown in Figure 5. Each cycle corresponds to a shed vortex. Considerable variation occurs in the peak-to-peak sensor signal at a given flow condition.

To ensure reliable detection of shed vortices, the sensor signal should at all times be maintained at an amplitude greater than the threshold of the signal conditioner. Otherwise some vortices will not be detected, and volumetric flow accuracy will be degraded. Therefore, all data in this section are presented in terms of the observed minimum peak-to-peak sensor signal V_S.

The dependence of V_S on connecting tubing geometry was measured. With the volumetric flow, density, and tubing internal diameter as constants, the tubing length was varied incrementally. V_S was found to vary approximately as $1/\sqrt{\ell}$. Similarly, for constant tubing length, the variation of V_S with tubing internal diameter from 0.16 to 0.64 cm was determined. V_S was found to vary directly as the diameter d.

Other measurements were made to determine V_S as a function of ρ and q. Knowledge of such a relationship would permit extrapolation of V_S over the entire range of flow conditions in this application. The variation of V_S with air flow at two densities is shown in Figure 6. The shapes of these curves are typical of all the data. At all flows, as density increases, V_S increases. However, no well-defined relationship could be established for V_S as a function of density. Evidently the three factors that determine sensitivity (the amplitude of vortex-generated pressure pulses, sensor thermal response, and connecting tube geometry) interact in a complicated manner as the density is varied.

Since signal performance could not be extrapolated from the air flow tests to the low-density helium flow conditions, signal performance was determined from tests with helium.

The variation of V_S with helium flow at 0.1 and 0.4-MPa and 10°C is shown in Figure 7. At this temperature the density of helium at 0.1 MPa is approximately equivalent to its density at 0.2 MPa and 350°C, the low-density condition in the application. The 0.1-and 0.4-MPa curves show the strong dependence of V_S upon density at low to medium volumetric flow rates. At the 0.4-MPa pressure, V_S remained above threshold down to $R_D = 6000$, and down to $R_D = 9000$ at the 0.1-MPa condition.

The relative sensitivity of the flowmeter to helium versus air can be estimated by comparison of Figures 6 and 7. Both the curve for air at $\rho = 2.59$ kg/m^3 and the curve for helium at $\rho = 0.68$ kg/m^3 have a peak V_S at approximately 17-18 mV p-p. Taking into account the relative densities, we estimate that the sensitivity to helium is approximately 3.4 times that of air. Therefore, lower flow rates of helium can be measured than of air.

shown in Figure 6. The shapes of these curves are typical of all the data. At all flows, as density increases, V_S increases. However, no well-defined relationship could be established for V_S as a function of density. Evidently the three factors that determine sensitivity (the amplitude of vortex-generated pressure pulses, sensor thermal response, and connecting tube geometry) interact in a complicated manner as the density is varied.

Since signal performance could not be extrapolated from the air flow tests to the low-density helium flow conditions, signal performance was determined from tests with helium.

The variation of V_S with helium flow at 0.1 and 0.4-MPa and 10°C is shown in Figure 7. At this temperature the density of helium at 0.1 MPa is approximately equivalent to its density at 0.2 MPa and 350°C, the low-density condition in the application. The 0.1-and 0.4-MPa curves show the strong dependence of V_S upon density at low to medium volumetric flow rates. At the 0.4-MPa pressure, V_S remained above threshold down to $R_D = 6000$, and down to $R_D = 9000$ at the 0.1-MPa condition.

The relative sensitivity of the flowmeter to helium versus air can be estimated by comparison of Figures 6 and 7. Both the curve for air at $\rho = 2.59$ kg/m^3 and the curve for helium at $\rho = 0.68$ kg/m^3 have a peak V_S at approximately 17-18 mV p-p. Taking into account the relative densities, we estimate that the sensitivity to helium is approximately 3.4 times that of air. Therefore, lower flow rates of helium can be measured than of air.

During the tests with air, the gas temperatures were raised to as high as 290°C. A thermocouple in the sensor block measured the block temperature. An equilibrium block temperature rise of only 9°C above ambient (23°C) was measured with the air at 290°C.

Rangeability is defined as the ratio of the maximum to the minimum volumetric flow for which V_S remains above the signal conditioner threshold. For air flow, a rangeability of 160:1 was demonstrated at $\rho = 5.18$ kg/m^3 in these tests (see Figure 6). This represents a volumetric flow range of 0.143 to 22.80 actual m^3/min, which corresponds to a vortex shedding rate of 2.5 to 400 Hz and an R_D range from 9×10^3 to 1.44×10^6. This rangeability represents the limitations of the test loop. A considerably wider rangeability was demonstrated during later calibration of the VSFM at the CEES.

FLOWMETER DESIGN

The results of development work discussed in the previous section indicated that a VSFM could be designed to meet all requirements in a single meter. Therefore, a VSFM was designed and fabricated for the GCFR test loop.

Design Rationale

The rationale of the design was to modify and enhance the Eastech design to meet the requirements and, to the extent possible, to assemble proven commercial components into a device with a greatly extended measurement capability. In addition to design criteria

stemming from developmental results, specific GCFR test loop operational, economic, and configuration constraints affected the design.

One significant constraint is the requirement that the entire GCFR test loop be covered with 2 in. of Kaowool insulation. Access to the insulation valves is required to change a sensor without venting the entire loop inventory of helium. However, in the Eastech design the valves are located in the connecting tubing runs, which would be beneath the surface of the loop insulation. Therefore, to minimize the length of the sensor connecting tubing, the sensor isolation valves must be installed in the sensor block rather than the connecting tubing. This meant redesign of the Eastech sensor mounting block.

During developmental testing, the Eastech press-fit mounting of the bluff body in the wafer body was found to be inadequate for high-temperature use, because at high temperatures the bluff body changed position sufficiently that all signal was lost. An alternative commercial mounting design that employs a removable bluff body could not meet GCFR test loop pressure boundary criteria. Therefore, a bluff body mounting mechanism was required that would be compatible with loop pressure boundary criteria and would provide alignment even at high temperatures.

To achieve maximum flow measurement accuracy, a smooth metering run equivalent in length to 40 pipe diameters upstream from the bluff body was required. The required downstream metering run was equivalent to 7 pipe diameters. Because of these requirements, and to minimize potential helium leaks in the loop at high pressures, the bluff body was permanently mounted in a long length of loop piping. The ends were permanently welded into the loop piping runs to eliminate costly flanges.

Finally, since the response curves for Eastech thermal sensor assemblies vary widely, and to also achieve maximum flow rangeability, sensors were selected to give responses that would match the signal conditioner response over the GCFR test loop flow and density ranges.

Design Description

The general features of the Eastech VSFM design are shown in Figure 8 and the GCFR test loop VSFM design is presented in Figure 9.

In the GCFR test loop design, the bluff body is precisely aligned in three degrees of freedom by dowels. The dowel holes in the meter body wall are sealed by welding from the outer pipe wall surface. The connecting tubing is welded at one end to the pipe wall, and at the other end to the sensor mounting block. The sensor mounting block incorporates integral sensor isolation valves. Valve seats in the block preserve the smoothness of the pressure pulse path to minimize signal noise. The valves, obtained from Autoclave Engineering, Inc., have high-pressure stems with multiple metal packing glands.

CALIBRATION

The linearity, accuracy, and rangeability of the four VSFMs assembled were calibrated at

[redacted] pipe diameters upstream from the bluff body was required. The required downstream metering run was equivalent to 7 pipe diameters. Because of these requirements, and to minimize potential helium leaks in the loop at high pressures, the bluff body was permanently mounted in a long length of loop piping. The ends were permanently welded into the loop piping runs to eliminate costly flanges.

Finally, since the response curves for Eastech thermal sensor assemblies vary widely, and to also achieve maximum flow rangeability, sensors were selected to give responses that would match the signal conditioner response over the GCFR test loop flow and density ranges.

Design Description

The general features of the Eastech VSFM design are shown in Figure 8 and the GCFR test loop VSFM design is presented in Figure 9.

In the GCFR test loop design, the bluff body is precisely aligned in three degrees of freedom by dowels. The dowel holes in the meter body wall are sealed by welding from the outer pipe wall surface. The connecting tubing is welded at one end to the pipe wall, and at the other end to the sensor mounting block. The sensor mounting block incorporates integral sensor isolation valves. Valve seats in the block preserve the smoothness of the pressure pulse path to minimize signal noise. The valves, obtained from Autoclave Engineering, Inc., have high-pressure stems with multiple metal packing glands.

CALIBRATION

The linearity, accuracy, and rangeability of the four VSFMs assembled were calibrated at an NBS-certified calibration facility, the CEES. This facility was chosen because it could calibrate the units over the entire GCFR test loop ranges of flow and density. The meter factor K was determined for the three 4-in. meters, FE-4, -7, and -9, and for the one 6-in. meter, FE-11.

Calibration System Description

The volumetric flow accuracy of the four meters was measured at the CEES over the range of conditions shown in Table I.

The calibration system is illustrated in Figure 10. The calibration loop consisted of three principal portions: (1) a helium supply from a high-pressure tube trailer; (2) a compressed air supply; and (3) a metering run with the VSFM in series with a standard, which was a critical venturi based on the Smith-Matz design. Both the primary sensor signal and the signal conditioner output were monitored with a dual-trace oscilloscope during the entire calibration.

For the low-density tests, the positions of the VSFM and the critical venturi were transposed. A silencer was located between the two flowmeters to attenuate any acoustic noise generated by the venturi. No acoustic noise was observed.

Table I. Conditions for calibration conducted at Colorado Engineering Experiment Station

Fluids	Compressed air Helium gas
Density	0.15 to 7.1 kg/m^3 (9.3×10^{-3} to 4.3×10^{-1} lb/ft^3)
Pipe Reynolds Number	5.9×10^3 to 1.7×10^6
Temperature	10 to 25°C

Calibration Procedure

Each calibration test was conducted by varying the pressure (and therefore the mass flow rate) at the critical venturi to obtain the desired VSFM flow range while the density was maintained constant at the VSFM. A value of the meter factor K for the VSFM was computed for each data point taken, using the following equations:

$$q_2 = \frac{\rho_1}{\rho_2} q_1 \tag{1}$$

and

$$K = \frac{60f}{q_2}, \tag{2}$$

where

ρ_1 = density at the venturi in kg/m^3 computed from pressure P_1 and temperature T_1,
q_1 = actual volumetric flow rate through the venturi, m^3/min,
q_2 = actual volumetric flow rate through the VSFM, m^3/min,
ρ_2 = density at the VSFM in kg/m^3 computed from pressure P_2 and temperature T_2,
f = frequency of vortex shedding from the VSFM, Hz,
K = meter factor of VSFM, cycles/actual m^3.

Calibration Results

Statistical analysis requires that many data points be obtained over the calibration range to establish the meter factor K for each meter. However, calibration of all four VSFMs over their entire range in the open loop at the CEES would have required an excessively large quantity of helium. Therefore, to conserve helium, data obtained with both air and helium gas flows were used to establish K. Also, since the three 4-in. VSFMs were constructed to the same dimensions within close tolerances, FE-4 was calibrated with helium and air, and FE-7 and -9 were calibrated with air alone. To obtain K for helium [illegible] the calibration data for FE-4 were compared with their air flow data.

computed for each data point taken, using the following equations:

$$q_2 = \frac{\rho_1}{\rho_2} q_1 \qquad (1)$$

and

$$K = \frac{60f}{q_2} , \qquad (2)$$

where

ρ_1 = density at the venturi in kg/m^3 computed from pressure P_1 and temperature T_1,
q_1 = actual volumetric flow rate through the venturi, m^3/min,
q_2 = actual volumetric flow rate through the VSFM, m^3/min,
ρ_2 = density at the VSFM in kg/m^3 computed from pressure P_2 and temperature T_2,
f = frequency of vortex shedding from the VSFM, Hz,
K = meter factor of VSFM, cycles/actual m^3.

Calibration Results

Statistical analysis requires that many data points be obtained over the calibration range to establish the meter factor K for each meter. However, calibration of all four VSFMs over their entire range in the open loop at the CEES would have required an excessively large quantity of helium. Therefore, to conserve helium, data obtained with both air and helium gas flows were used to establish K. Also, since the three 4-in. VSFMs were constructed to the same dimensions within close tolerances, FE-4 was calibrated with helium and air, and FE-7 and -9 were calibrated with air alone. To obtain K for helium for FE-7 and -9, the calibration data for FE-4 were compared with their air flow data.

All calibration data acquired on FE-4 for both air and helium flow are plotted in Figure 11. The data for both gases at the same density are plotted in Figure 12. Figure 13 shows the spread of the calibration data for air alone at two densities.

All calibration data from meter FE-4 acquired for helium flow alone are plotted in Figures 14-17. Next, all calibration data from meters FE-7 and -9 for air flow alone are presented in Figures 18 and 19. All calibration data for the 6-in. VSFM, FE-11, are plotted in Figure 20.

Accuracy/Rangeability

Flow measurement accuracy and rangeability are interrelated. Accuracy is defined as the nominal ($\pm 2\sigma$) accuracy of the meter. Rangeability relative to the sensor signal, as defined in the section on Remote Sensor Signal Performance, was demonstrated to be 348:1

at the CEES. This is the full operating range of the four GCFR test loop VSFMs. However, the nominal accuracy of these meters was much better over the 166:1 range of use in the test loop than over their full operating range. The analysis of calibration data for each meter is summarized according to R_D range, density, and gas in Tables II-IV.

Table II gives the helium gas calibration data for FE-4. The nominal accuracy falls between 0.9 and 1.9%, depending on the density and R_D ranges chosen. This accuracy-rangeability tradeoff is shown in Table V.

Table II. Calibration results for FE-4 with helium

No. of data points	Density (kg/m^3)	$\bar{K}$ (cycles/ACM)	σ (cycles/ACM)	$2\sigma/\bar{K}$ (%)	R_D range
12	0.154 (0.2 MPa equiv density)	1251.4	5.72	0.914	10^4 to 10^6
10	2.27 (3 MPa equiv density)	1244.5	7.17	1.153	10^4 to 10^6
13	6.73 (9 MPa equiv density)	1237.9	5.84	0.944	10^4 to 10^6
35	Composite	1244.4	8.35	1.342	10^4 to 10^6
52	Composite	1248.8	10.99	1.76	6×10^3 to 10^6
13	0.154	1257.7	11.81	1.88	6×10^3 to 10^4

Table III. Calibration results for FE-11 with air and helium

No. of data points	Density (kg/m^3)	Gas	$\bar{K}$ (cycles/ACM)	σ (cycles/ACM)	$2\sigma/\bar{K}$ (%)	R_D range
15	0.15 (0.2 MPa equiv	He	353.36	3.11	1.750	10^4 to 10^6

12	0.154 (0.2 MPa equiv density)	1251.4	5.72	0.914	10^4 to 10^6
10	2.27 (3 MPa equiv density)	1244.5	7.17	1.153	10^4 to 10^6
13	6.73 (9 MPa equiv density)	1237.9	5.84	0.944	10^4 to 10^6
35	Composite	1244.4	8.35	1.342	10^4 to 10^6
52	Composite	1248.8	10.99	1.76	6×10^3 to 10^6
13	0.154	1257.7	11.81	1.88	6×10^3 to 10^4

Table III. Calibration results for FE-11 with air and helium

No. of data points	Density (kg/m^3)	Gas	$\bar{K}$ (cycles/ACM)	σ (cycles/ACM)	$2\sigma/\bar{K}$ (%)	R_D range
15	0.15 (0.2 MPa equiv density)	He	353.36	3.11	1.750	10^4 to 10^6
9	0.77 (1.6 MPa equiv density)	He	359.60	1.96	1.091	10^4 to 10^6
26	7.07 (9 MPa equiv density)	Air	360.00	2.57	1.426	10^4 to 10^6
24	Composite	He	357.03	3.37	1.884	10^4 to 10^6

Table IV. Calibration results composite for 3- and 9-MPa equivalent densities

Meter	No. of data points	$\bar{K}$ (cycles/ACM)	σ (cycles/ACM)	$2\sigma/\bar{K}$ (%)	R_D range
FE-4	36	1248.7	7.20	1.154	10^4 to 10^6
FE-7	37	1249.8	7.17	1.148	10^4 to 10^6
FE-9	38	1245.9	10.10	1.620	10^4 to 10^6

Table V. Flow measurement accuracy/rangeability tradeoffs for FE-4 with He

	R_D
Case 1 - Separate K Factors	
0.2 MPa pressure	6×10^3 to 10^4
Each pressure (0.2, 3, and 9 MPa)	10^4 to 10^5
Resultant nominal accuracy:*	
1.9%	6×10^3 to 10^4
1.0%	10^4 to 10^6
Case 2 - Separate K Factors	
0.2 MPa pressure	6×10^3 to 10^4
Composite of all pressures	10^4 to 10^6
Resultant nominal accuracy:*	
1.9%	6×10^3 to 10^4
1.3%	10^4 to 10^6
Case 3 - Single Lumped K Factor	6×10^3 to 10^6
Resultant nominal accuracy:*	
1.8%	6×10^3 to 10^6

*Percent of reading.

tradeoffs for FE-4 with He

	R_D
Case 1 - Separate K Factors	
0.2 MPa pressure	6×10^3 to 10^4
Each pressure (0.2, 3, and 9 MPa)	10^4 to 10^5
Resultant nominal accuracy:*	
1.9%	6×10^3 to 10^4
1.0%	10^4 to 10^6
Case 2 - Separate K Factors	
0.2 MPa pressure	6×10^3 to 10^4
Composite of all pressures	10^4 to 10^6
Resultant nominal accuracy:*	
1.9%	6×10^3 to 10^4
1.3%	10^4 to 10^6
Case 3 - Single Lumped K Factor	6×10^3 to 10^6
Resultant nominal accuracy:*	
1.8%	6×10^3 to 10^6

*Percent of reading.

In Case 1 of Table V, four K factors are needed for each 4-in. meter. The result is a nominal accuracy of 1.9% in the R_D range from 6×10^3 to 10^4 at the GCFR test loop at 0.2 MPa pressure. The only GCFR test loop flows below an R_D of 10^4 occur at this low pressure. Above an R_D of 10^4, the accuracy is 1.0%.

For Case 2, there are two K factors for each 4-in. meter, one for 0.2 MPa pressure with R_D less than 10^4, and one for all pressures with R_D greater than 10^4. The resultant nominal accuracies are 1.9 and 1.3% respectively.

Case 3 represents the most general case. A single lumped K factor for each 4-in. meter for all pressures and for an R_D from 6×10^3 to 10^6 gives a nominal accuracy of 1.8%.

From the preceding discussion, it can be seen that there is a tradeoff between accuracy and rangeability. If high accuracy is required, the approach in Case 1 should be followed. Here, multiple K factors must be used over the full GCFR test loop range, with a means of associating each K factor with its applicable pressure and R_D range. To achieve a maximum flow rangeability at all GCFR test loop pressures using a single K factor, the approach in Case 3 should be followed. Compared with Case 1, the nominal accuracy is significantly degraded.

Recommended K Factors for GCFR Test Loop Use

To best meet the GCFR test loop requirement of a flow measurement accuracy of 1.0%, the K factors shown in Table VI are recommended. The accuracy requirement was met for the 4-in. meters throughout the most important portion of the GCFR test loop flow range. For FE-11 insufficient calibration data were collected to establish a K factor that would result in an accuracy better than 1.9%.

The method for constructing the curve of volumetric flow versus vortex shedding frequency using the K factor is given in Appendix A.

Table VI. Recommended K factors for GCFR test loop

CFTL meter	CFTL pressure (MPa)	Flow range, R_D	K Factor (cycles/ACM)	Nominal accuracy* (%)
FE-4	0.2	6×10^3 to 10^4	1257.7	1.9
	0.2	10^4 to 10^6	1251.4	1.0
	3.0	10^4 to 10^6	1244.5	1.0
	9.0	10^4 to 10^6	1237.9	1.0
FE-7	0.2	6×10^3 to 10^4	1258.9	1.9
	0.2	10^4 to 10^6	1252.6	1.0
	3.0	10^4 to 10^6	1245.7	1.0
	9.0	10^4 to 10^6	1239.1	1.0
FE-9	0.2	6×10^3 to 10^4	1254.9	1.9
	0.2	10^4 to 10^6	1248.6	1.0
	3.0	10^4 to 10^6	1241.7	1.0
	9.0	10^4 to 10^6	1235.1	1.0
FE-11	0.2, 3.0, 9.0	10^4 to 10^6	357.03	1.9

*Percent of reading.

OPERATIONAL PERFORMANCE

Two of the fabricated VSFMs, FE-4 and FE-11, have been in operation in the GCFR test loop since October 1981 at circulating gas temperatures up to 300°C. Both meters have per-

FE-4	0.2	6×10^3 to 10^4	1257.7	1.9
	0.2	10^4 to 10^6	1251.4	1.0
	3.0	10^4 to 10^6	1244.5	1.0
	9.0	10^4 to 10^6	1237.9	1.0
FE-7	0.2	6×10^3 to 10^4	1258.9	1.9
	0.2	10^4 to 10^6	1252.6	1.0
	3.0	10^4 to 10^6	1245.7	1.0
	9.0	10^4 to 10^6	1239.1	1.0
FE-9	0.2	6×10^3 to 10^4	1254.9	1.9
	0.2	10^4 to 10^6	1248.6	1.0
	3.0	10^4 to 10^6	1241.7	1.0
	9.0	10^4 to 10^6	1235.1	1.0
FE-11	0.2, 3.0, 9.0	10^4 to 10^6	357.03	1.9

*Percent of reading.

OPERATIONAL PERFORMANCE

Two of the fabricated VSFMs, FE-4 and FE-11, have been in operation in the GCFR test loop since October 1981, at circulating gas temperatures up to 300°C. Both meters have performed well and within design requirements.

In October 1982, an additional VSFM, FE-7, was installed. At that time the circulating gas temperature was increased to 450°C, placing the operating conditions well outside the design envelope of the meters. At this high circulating gas temperature, the sensor block temperature on FE-4 and FE-11 increased to 92°C, and to 198°C on FE-7. Under these conditions FE-4 and FE-11 performed only marginally, and FE-7 became very erratic and unusable. The primary problem was too high an ambient gas temperature around the thermal sensors, causing low signal-to-noise ratios and below threshold signal levels. Water cooling was introduced on each sensor block, and reliable meter operation was restored.

CONCLUSIONS

The full range GCFR test loop flow measurement requirements can be fulfilled with a modified VSFM having a remotely located thermal sensor, as demonstrated by a volumetric flow measurement accuracy of ±1.0% of reading over a flow range of 100:1. Over an extended range of greater than 167:1 in flow and 46:1 in density, an accuracy of ±1.8% of reading was demonstrated, and usable vortex shedding signals were observed over a 348:1 flow range.

APPENDIX A

Use of K Factor to Determine Volumetric Flow

The actual volumetric flow rate can be determined from the vortex shedding frequency by the following equation:

$$q = \frac{60}{K} f \ ,$$

where

q = actual volumetric flow rate, m^3/min,
K = meter factor of VSFM, cycles/actual m^3,
f = frequency of vortex shedding from VSFM, Hz.

Figure A-1 is a general plot of this equation. The slope of the curve is determined solely by the K factor. From this plot, the actual volumetric flow rate for a given vortex shedding rate can be determined graphically.

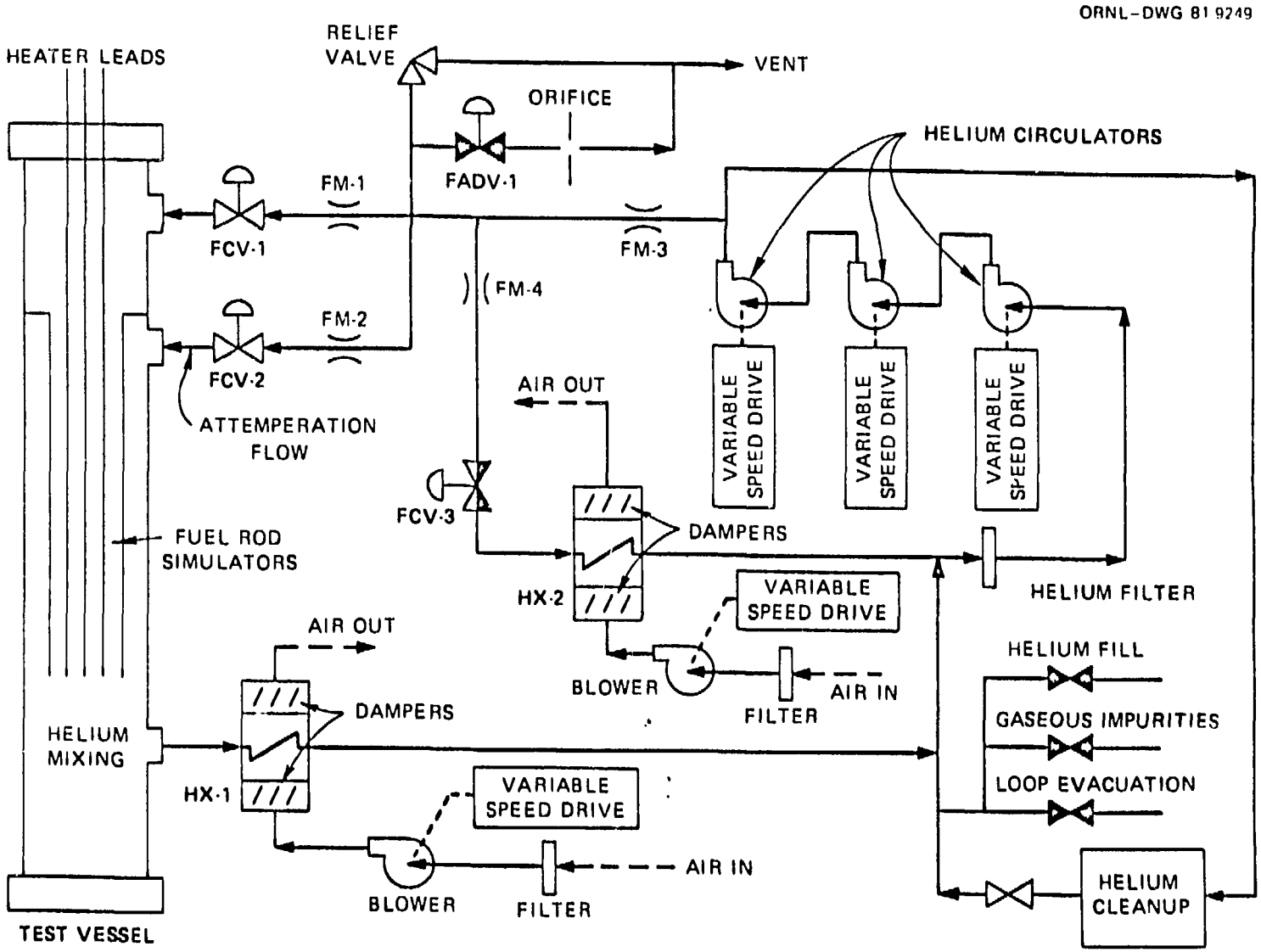

Figure 1. Flow diagram of GCFR test loop.

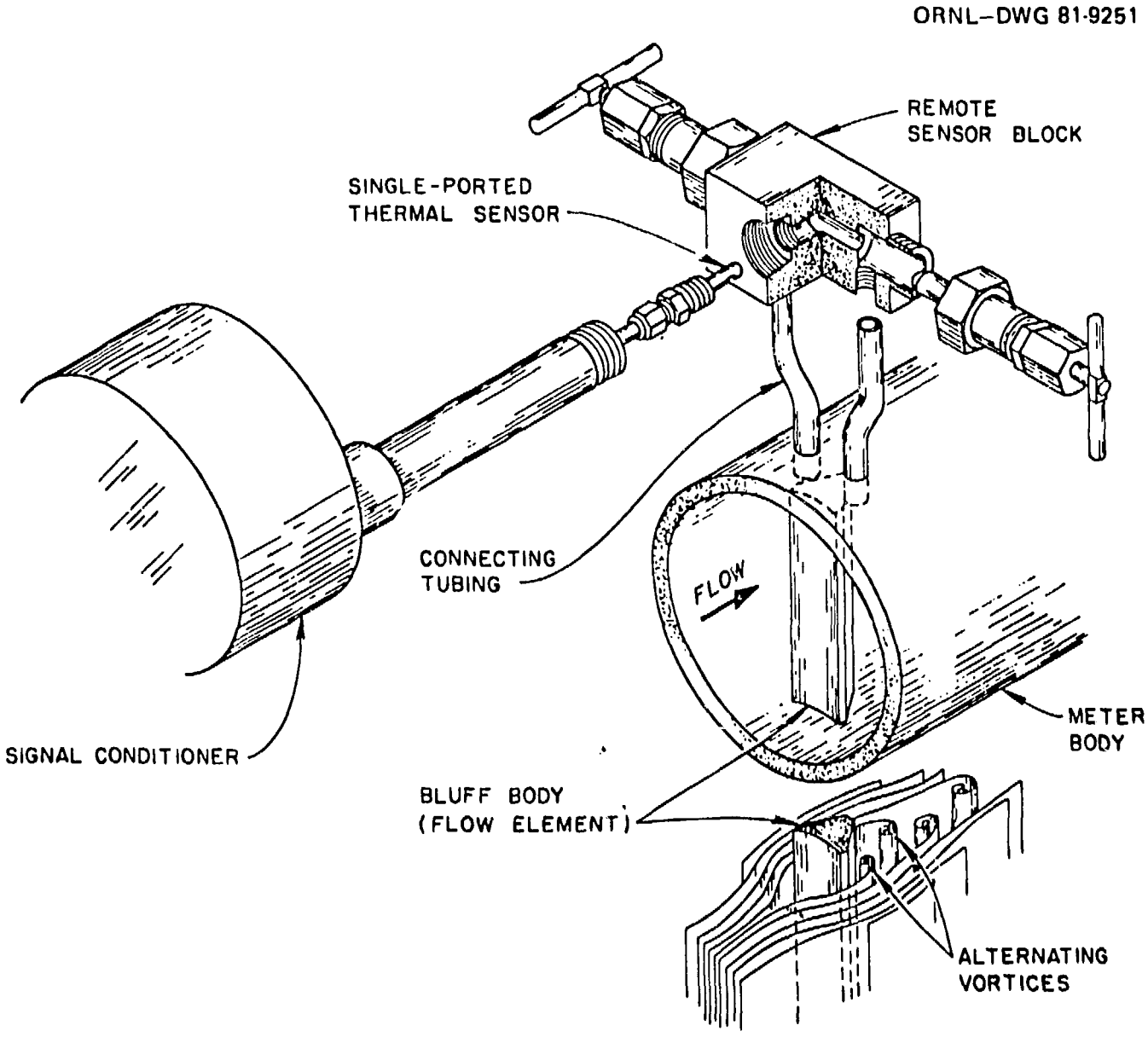

Figure 2. Modified VSFM.

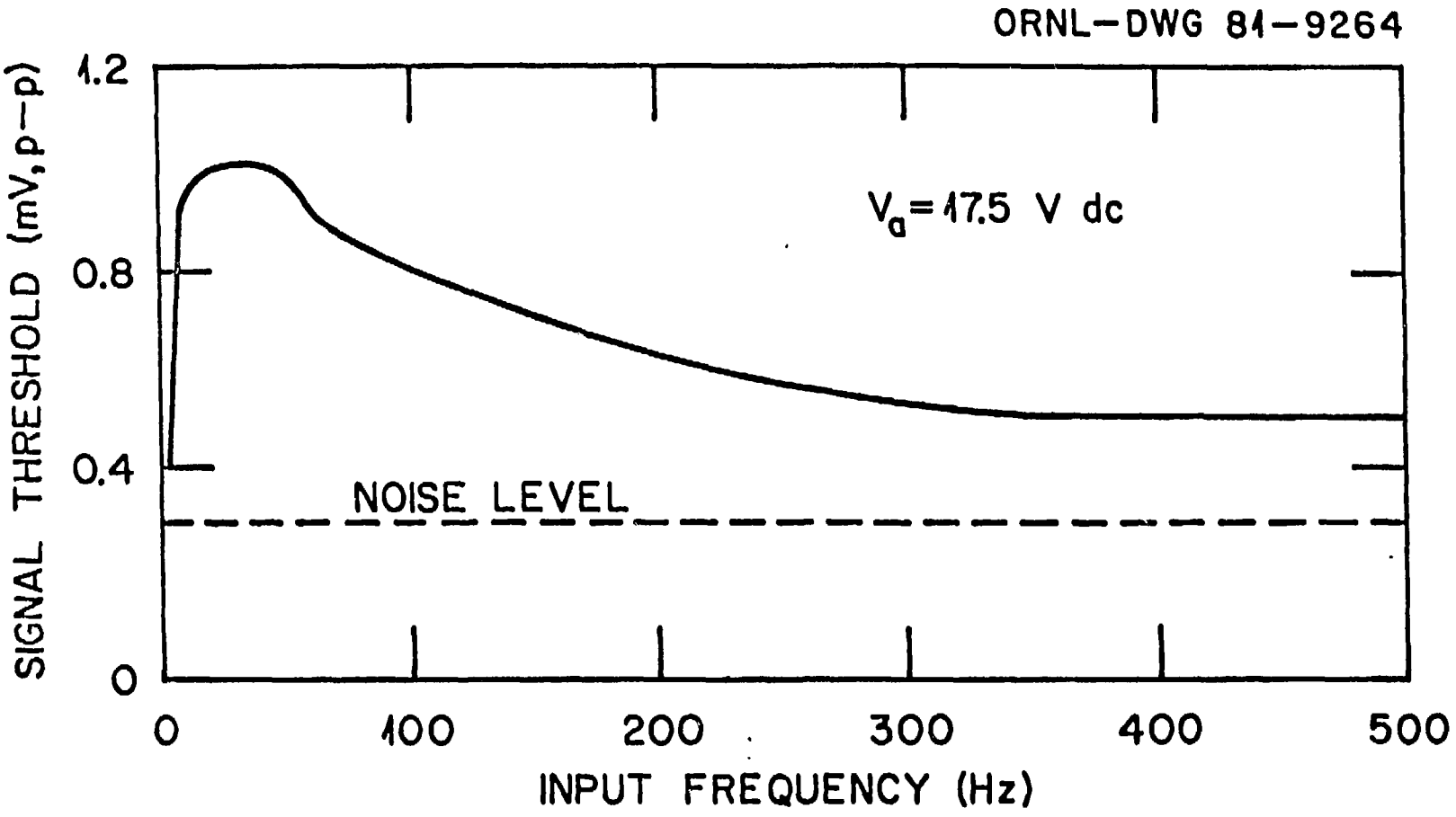

Figure 3. Threshold response of signal conditioner.

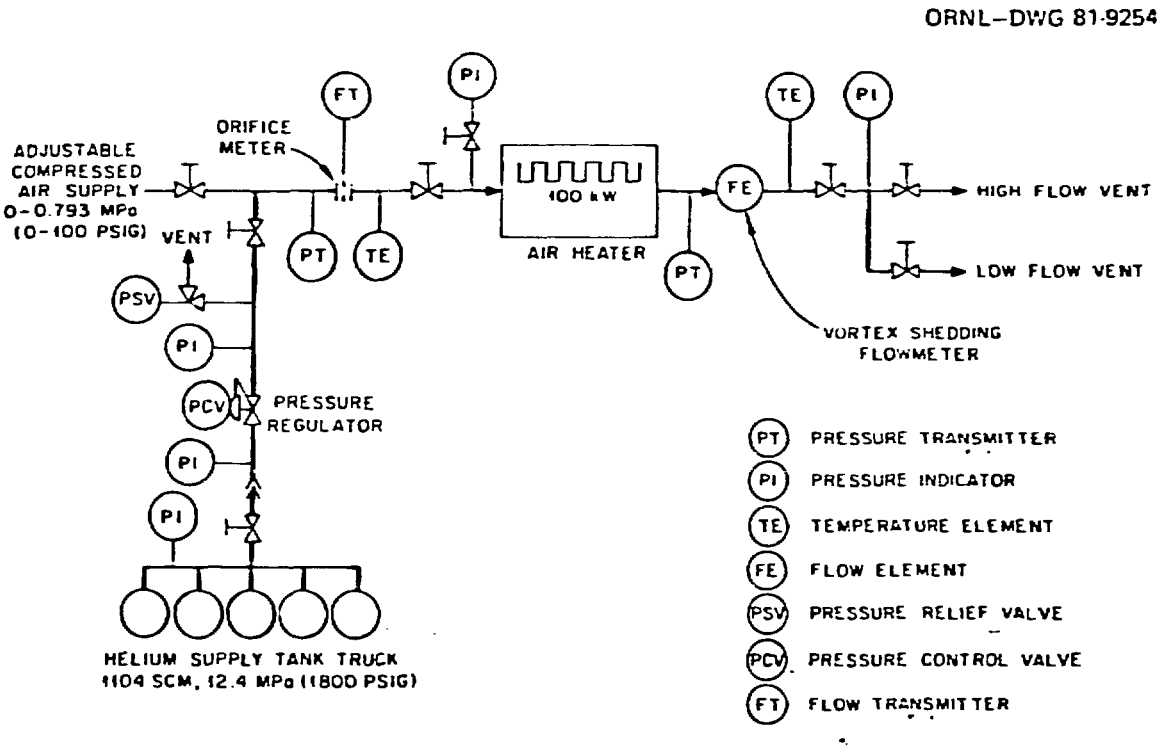

Figure 4. Test loop used for remote sensor signal measurements.

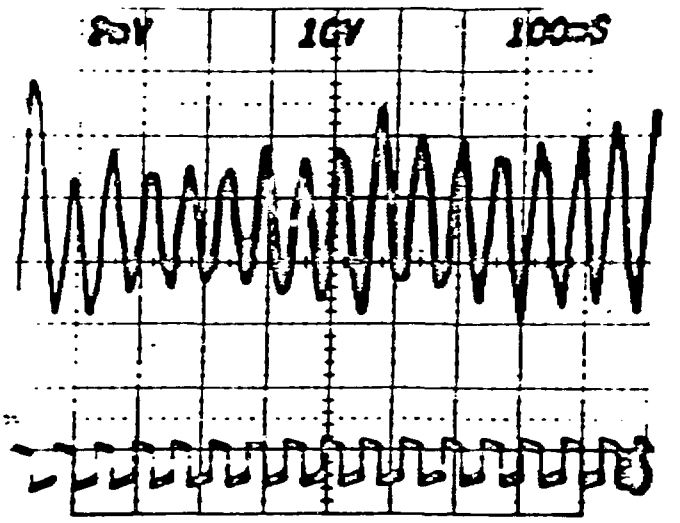

(*a*) LOW FLOW: VORTEX SHEDDING RATE = 15 Hz

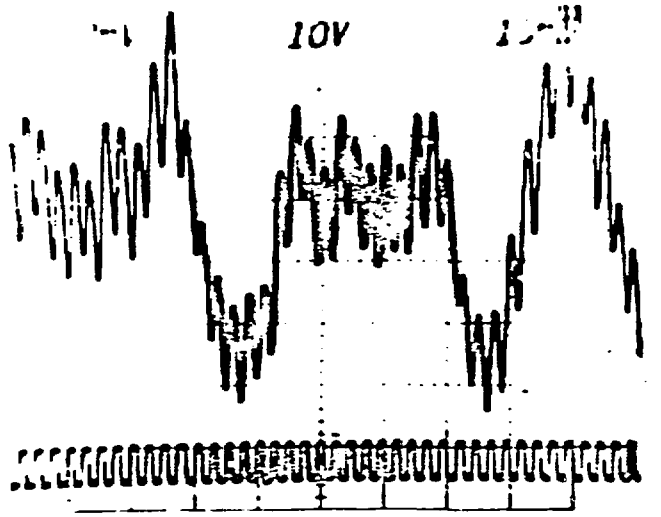

(*b*) HIGH FLOW: VORTEX SHEDDING RATE = 396 Hz

Figure 5. Oscilloscope trace of sensor output (channel 1) and signal conditioner output (channel 2).

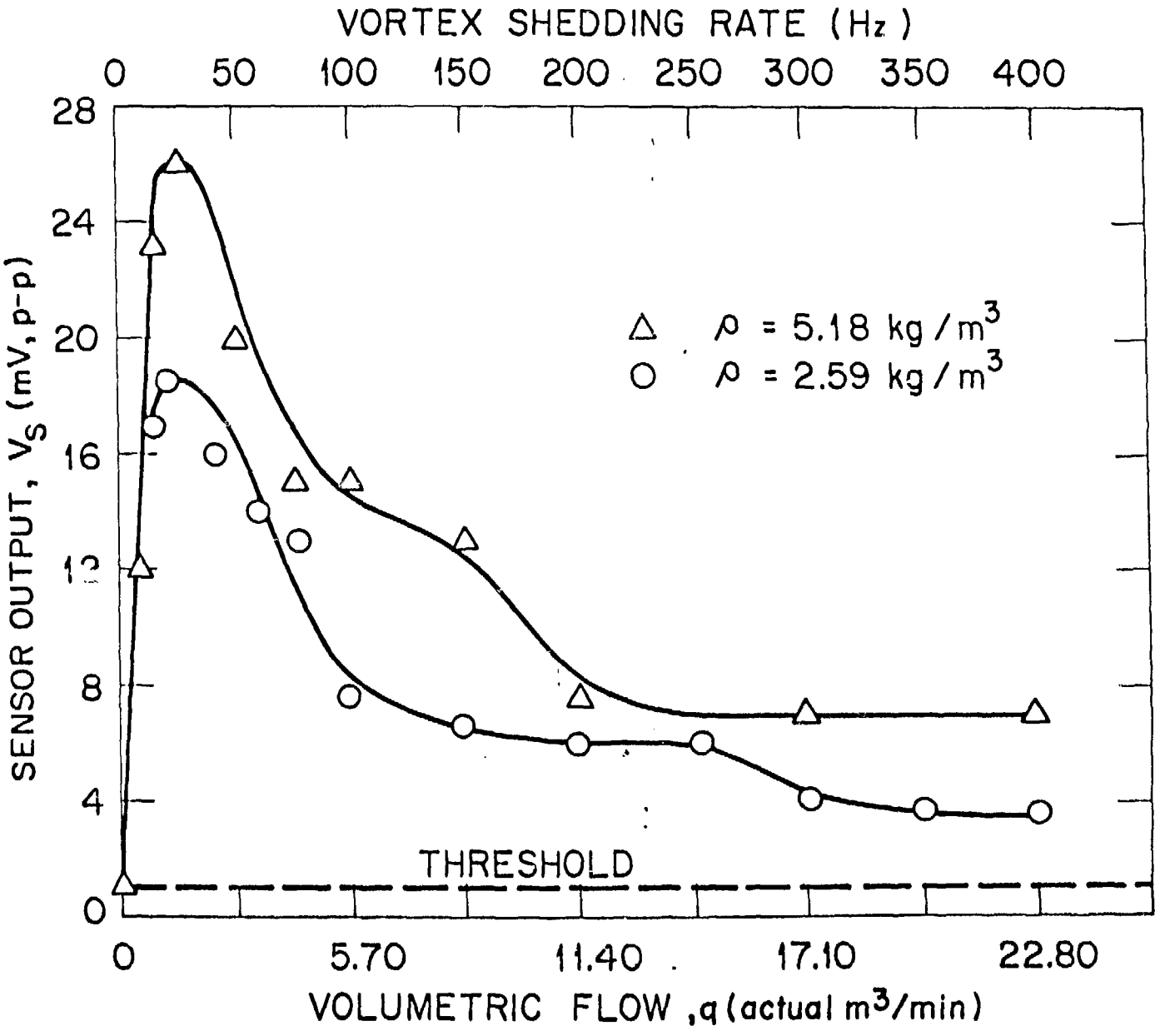

Figure 6. V_s versus air flow at constant densities.

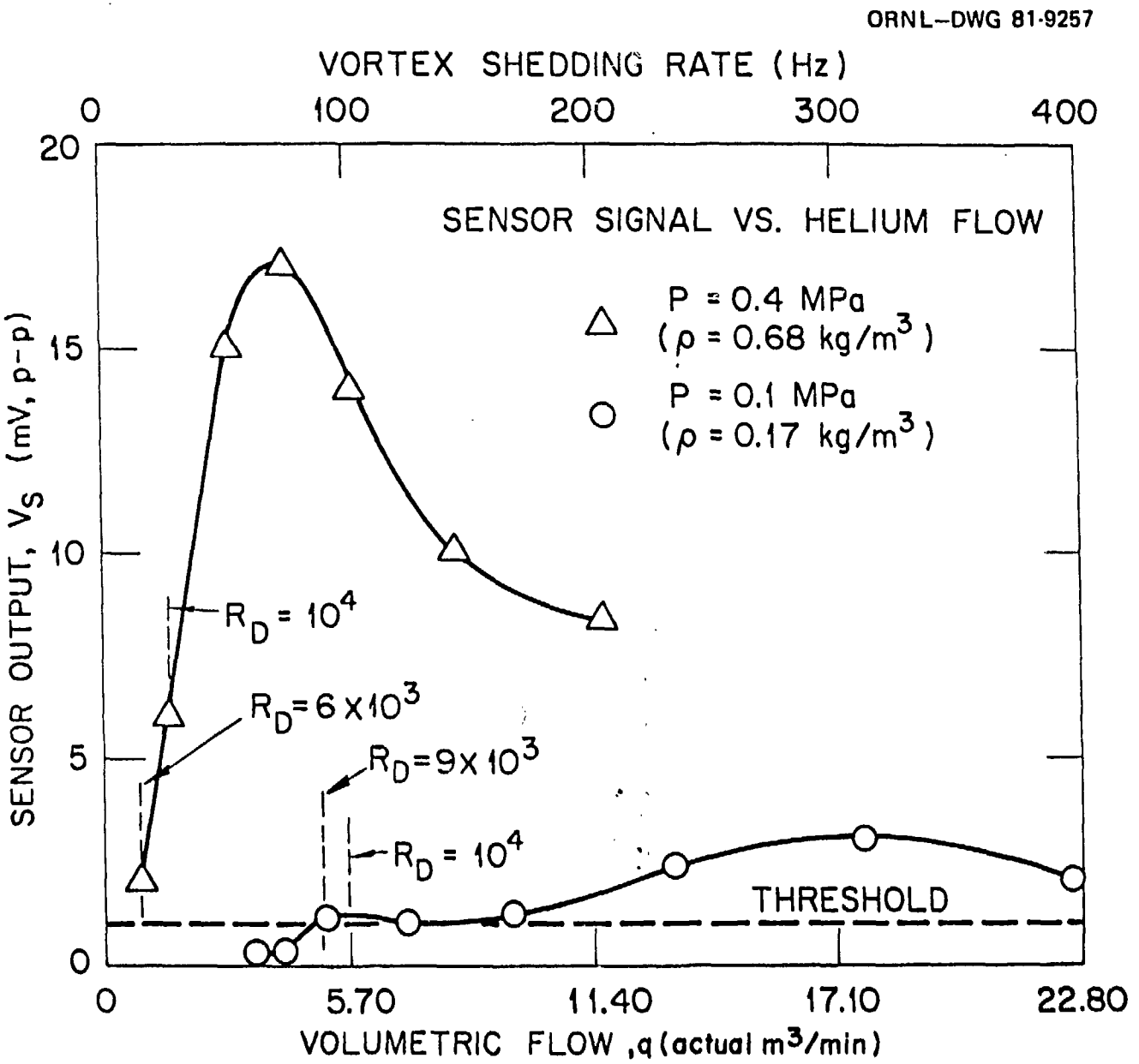

Figure 7. V_s versus helium flow at constant densities.

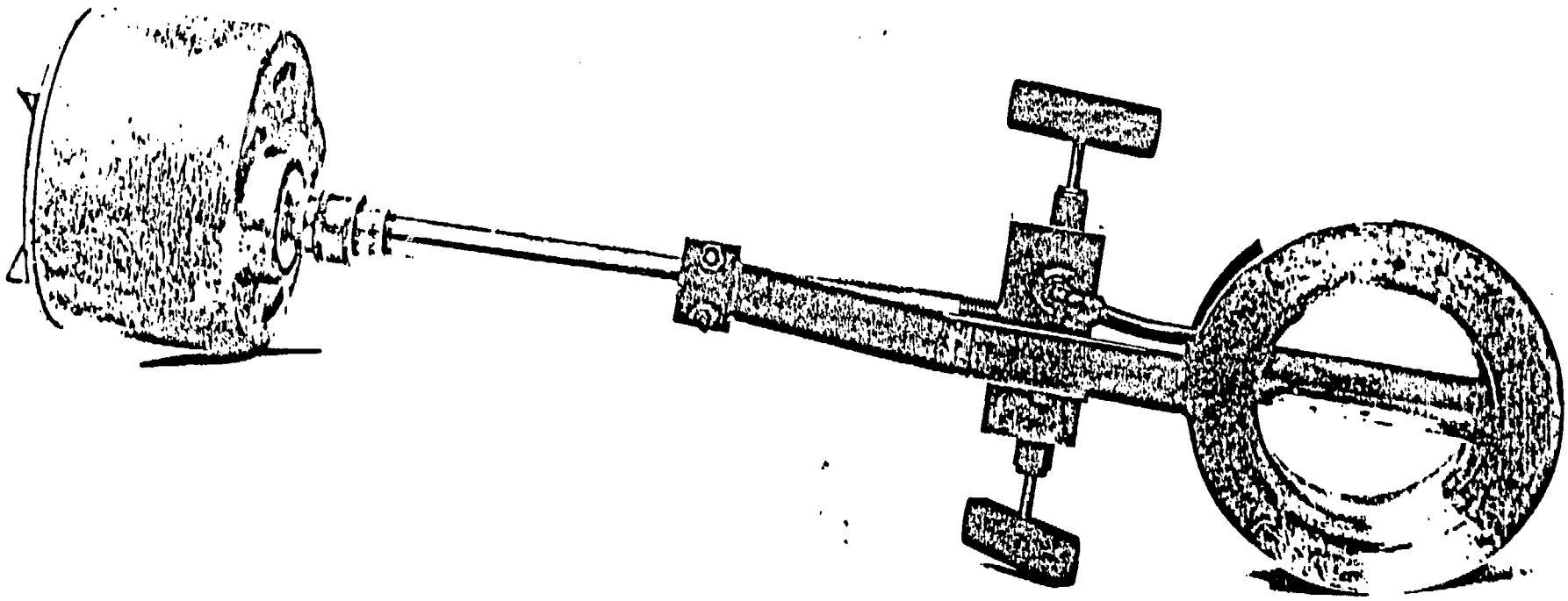

Figure 8. Photograph of wafer meter showing the main features of the Eastech VSFM design.

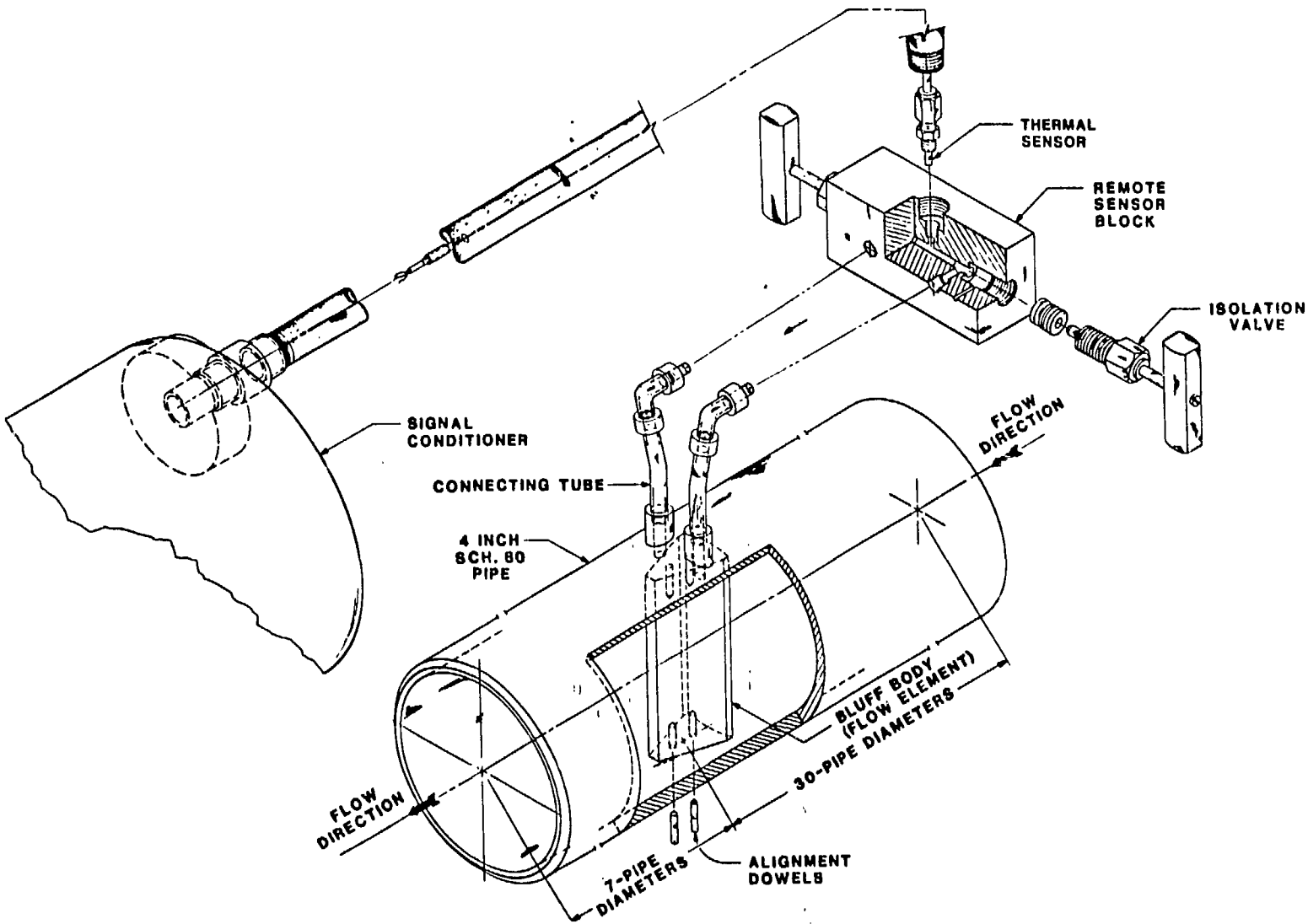

Figure 9. Design of the VSFM modified for use in the GCFR test loop.

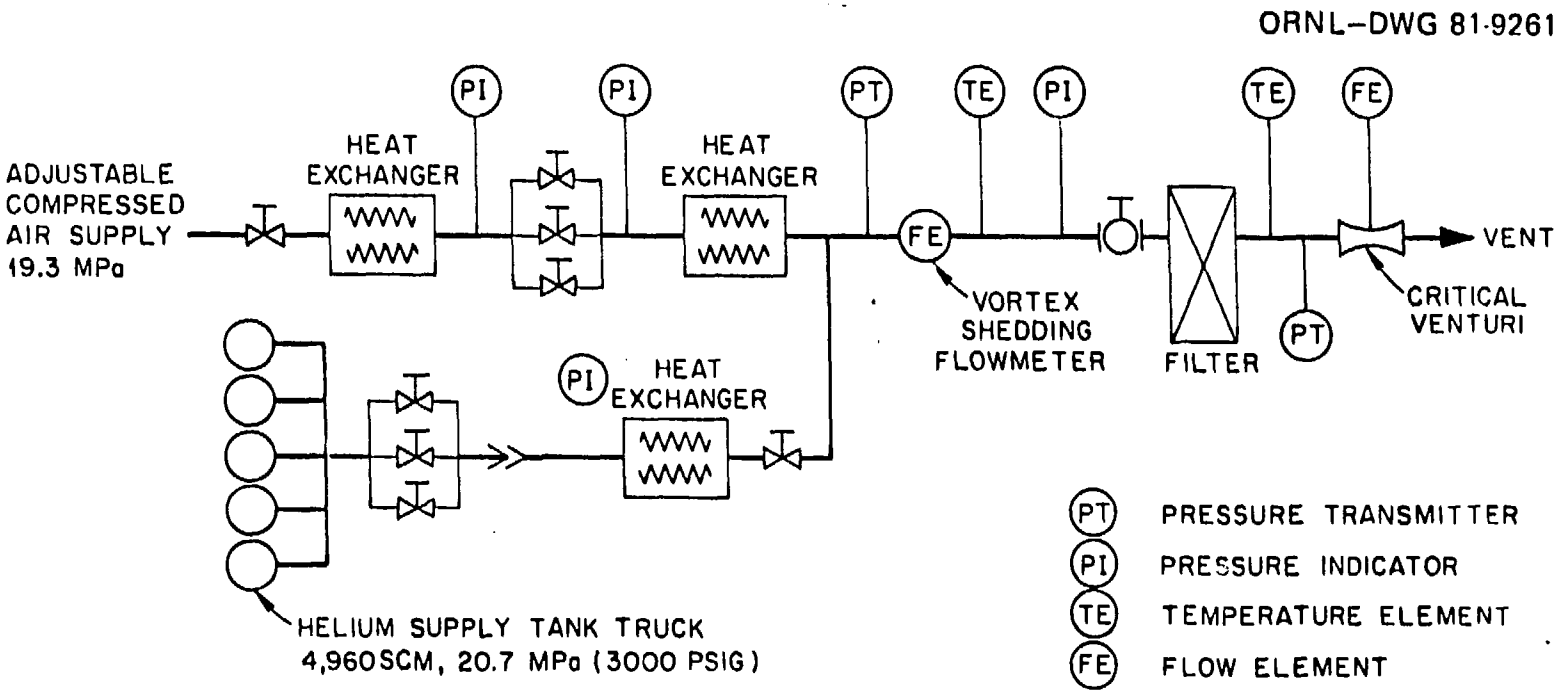

Figure 10. VSFM calibration system.

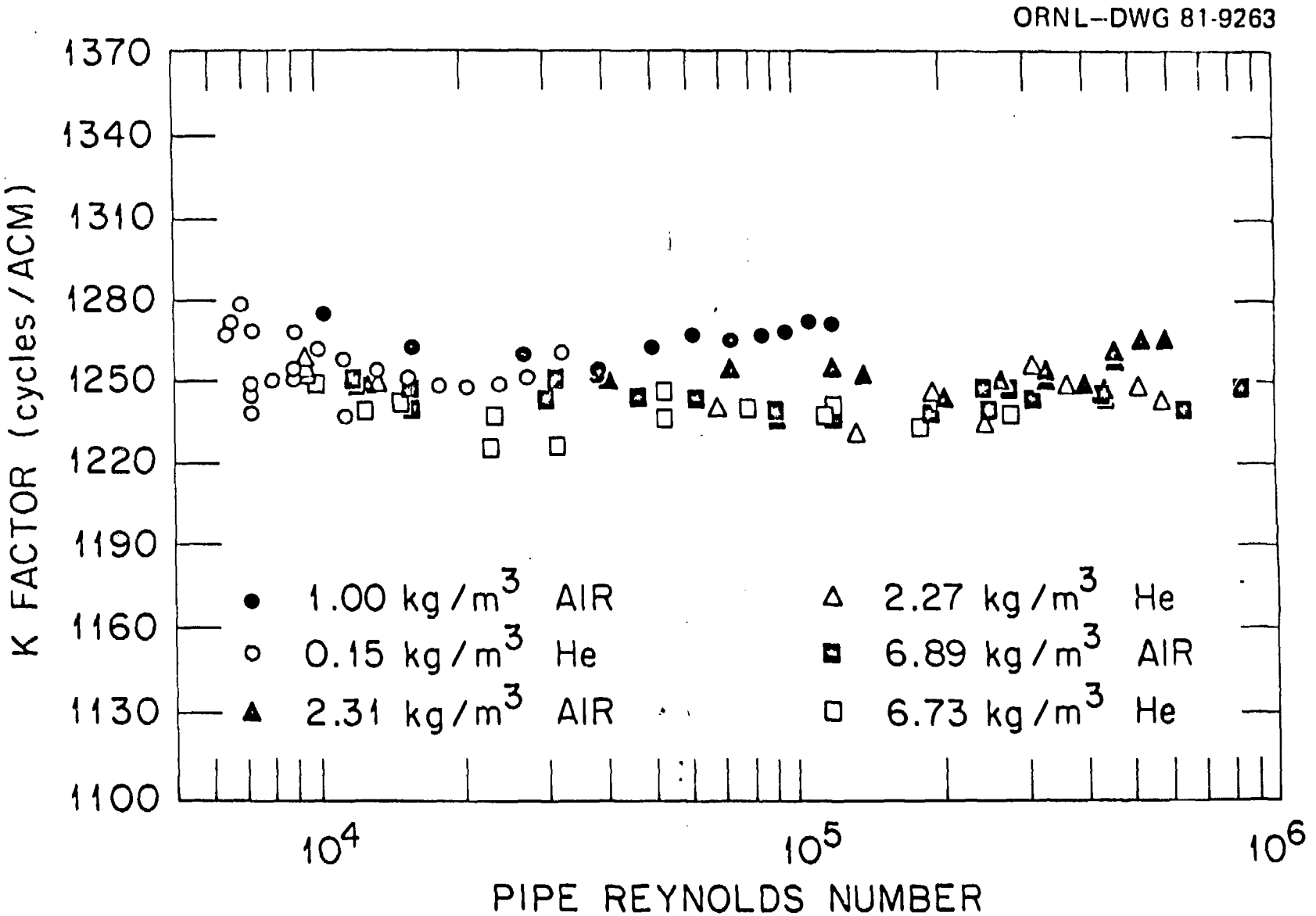

Figure 11. K factor versus Pipe Reynolds number for FE-4 (all calibration data).

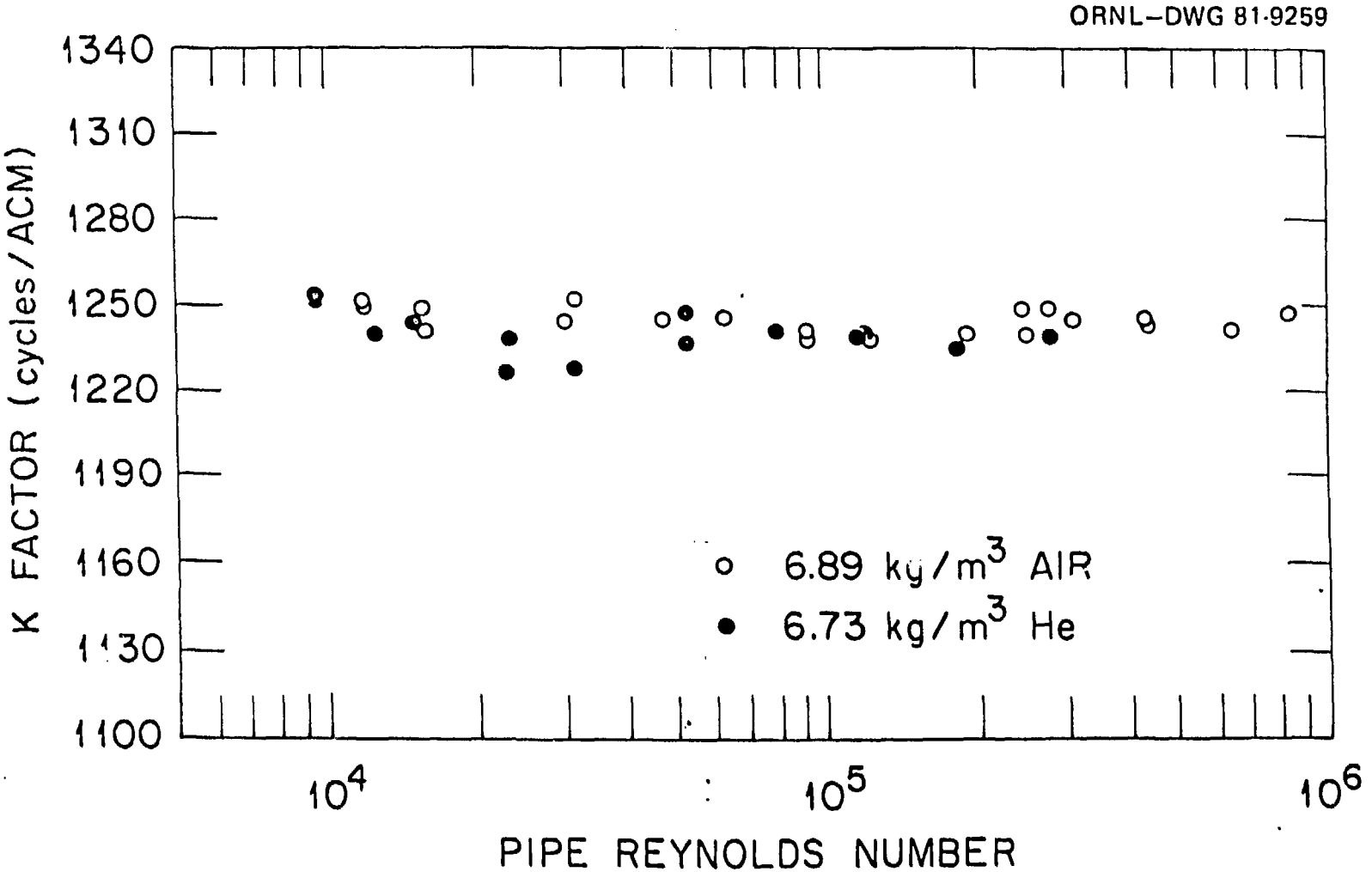

Figure 12. K factor versus Pipe Reynolds number for FE-4 (high-density air and helium).

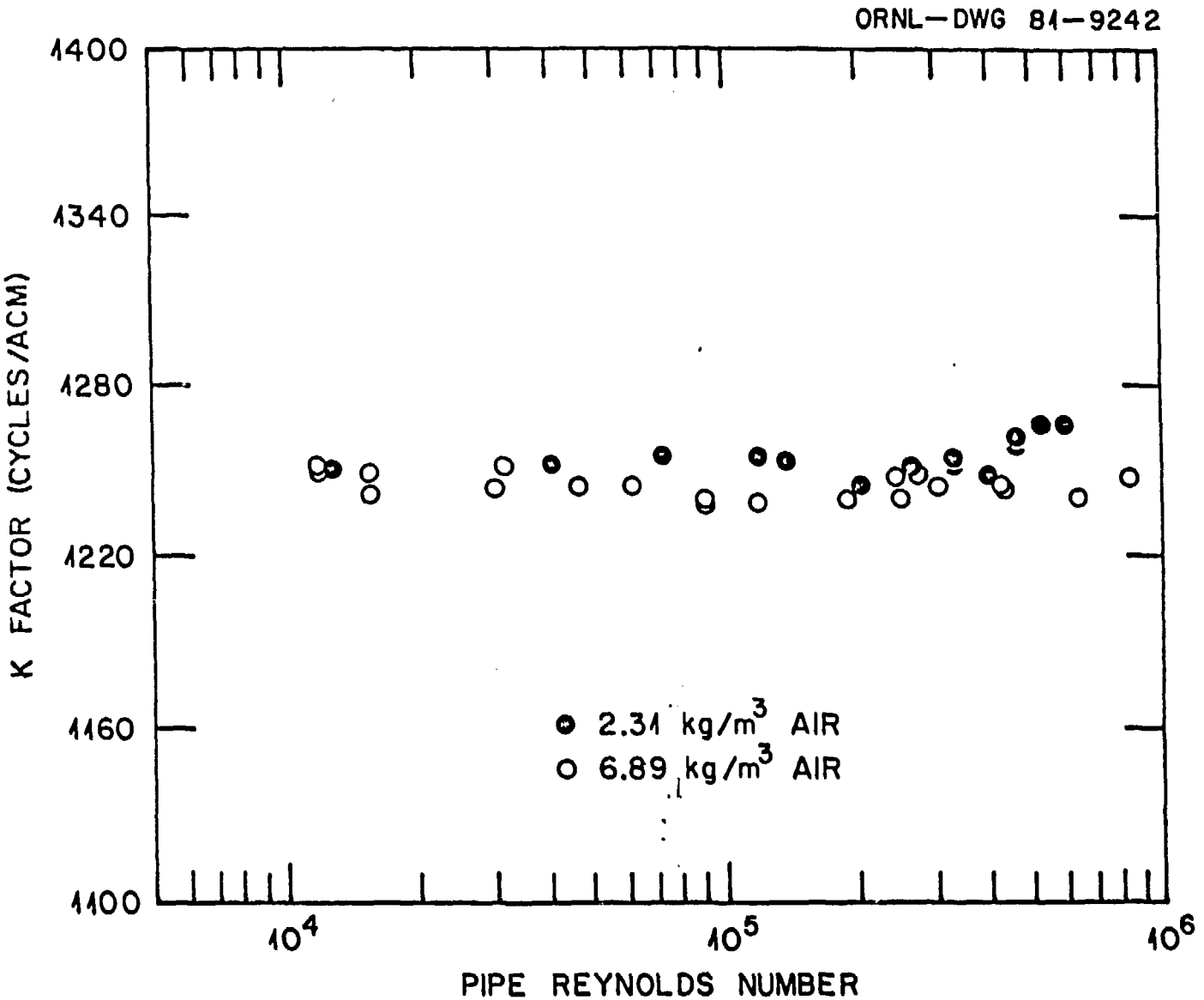

Figure 13. K factor versus Pipe Reynolds number for FE-4 (medium- and high-density air data).

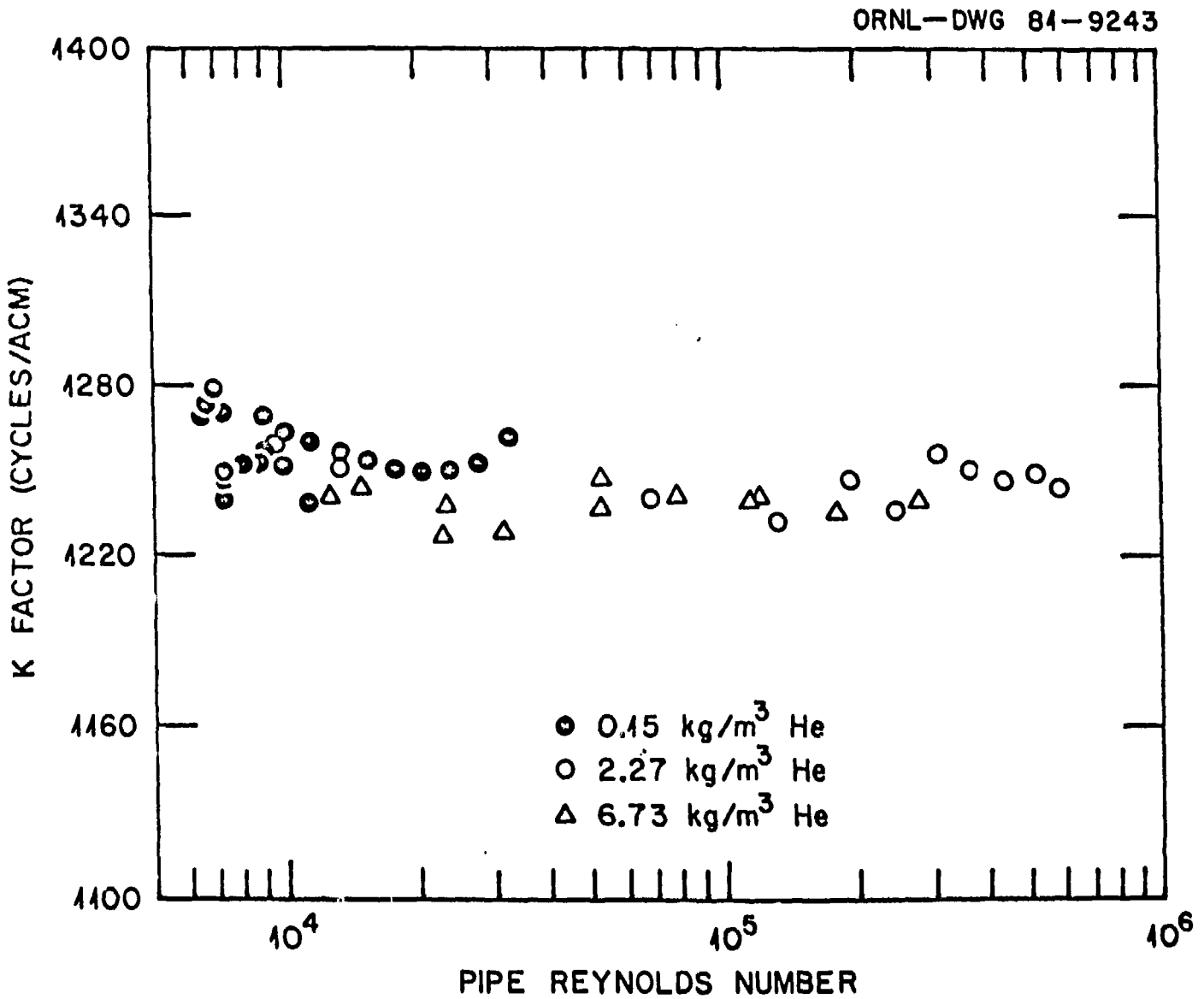

Figure 14. K factor versus Pipe Reynolds number for FE-4 (all helium data).

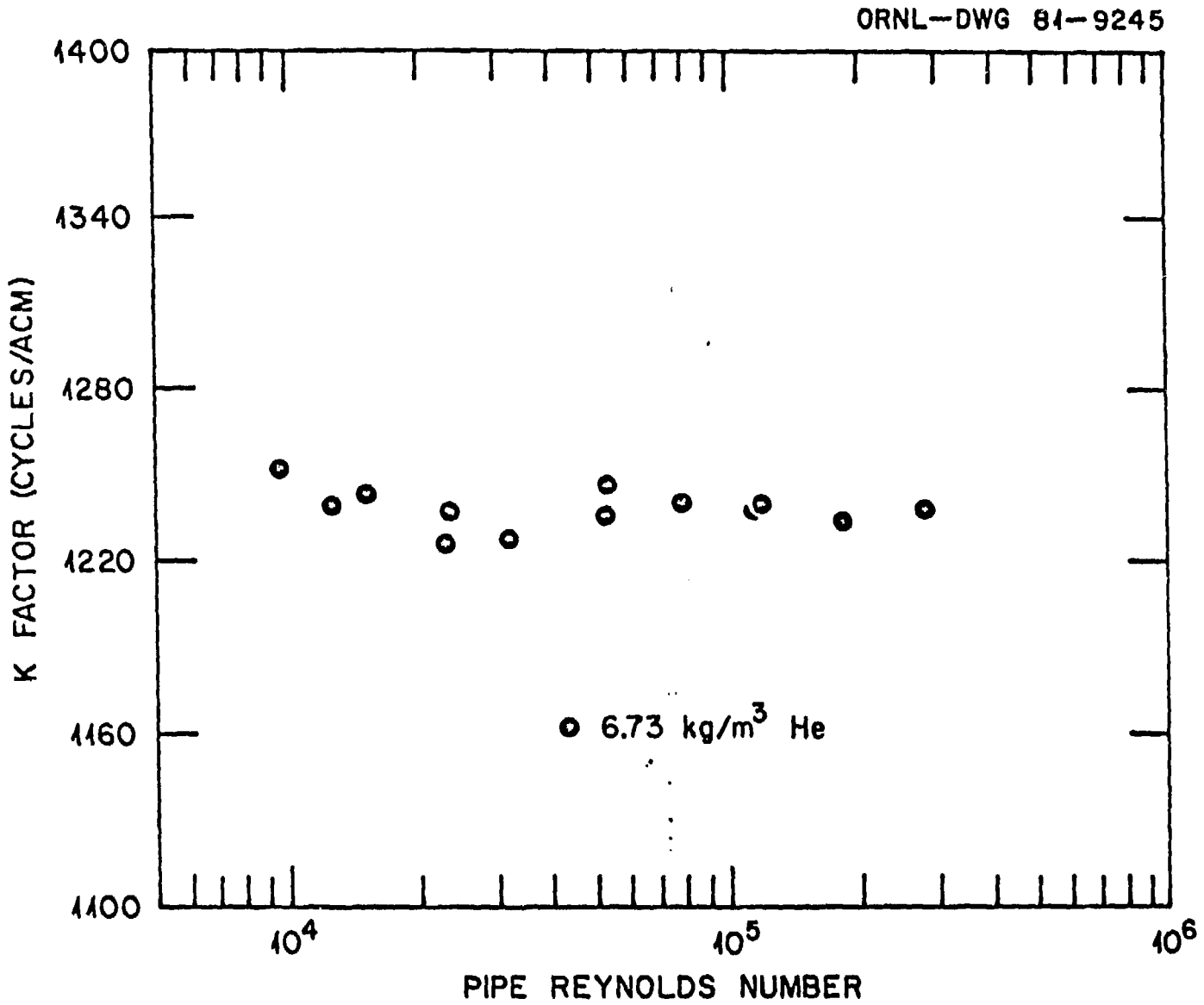

Figure 15. K factor versus Pipe Reynolds number for FE-4 (high-density helium data).

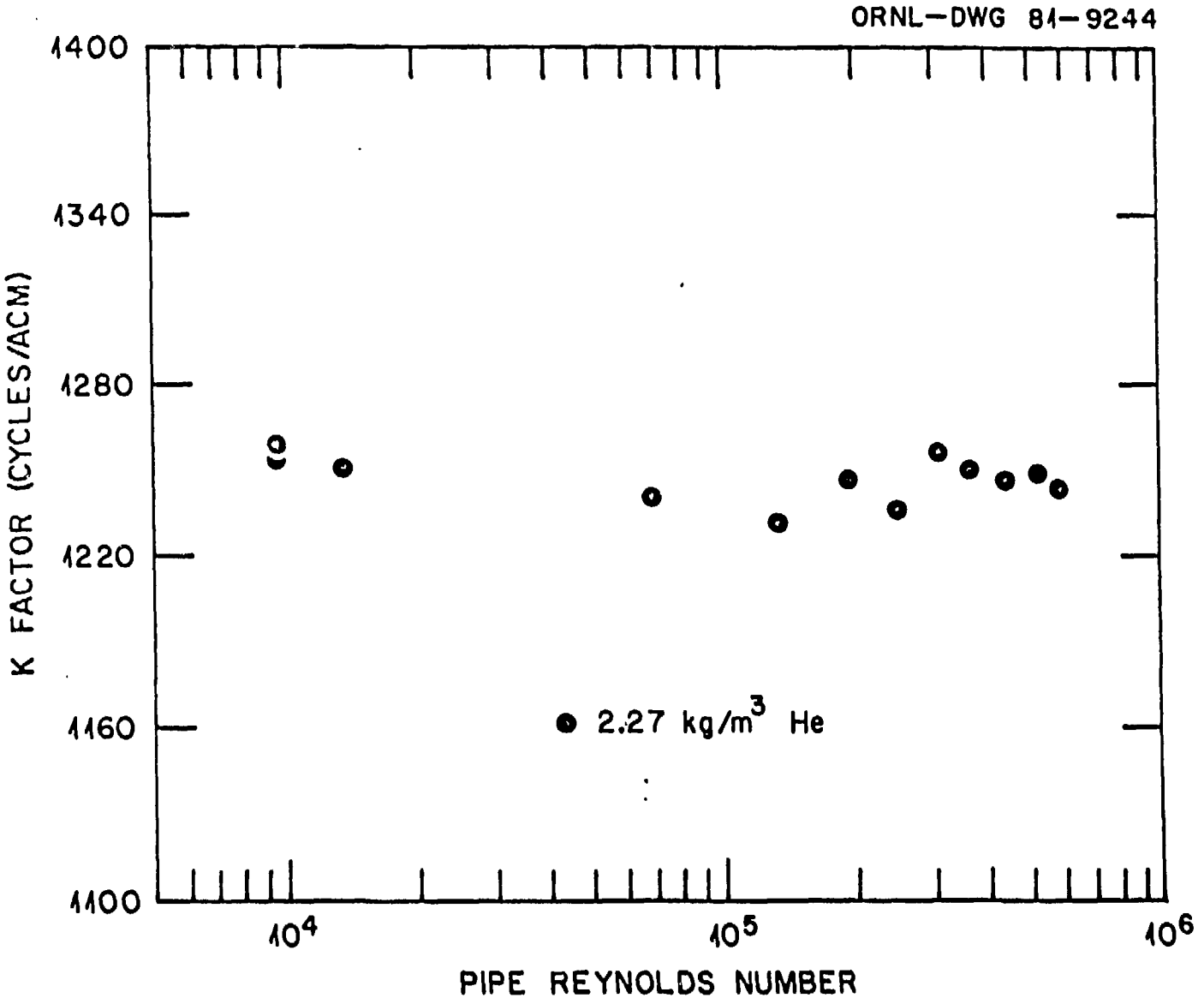

Figure 16. K factor versus Pipe Reynolds number for FE-4 (medium-density helium data).

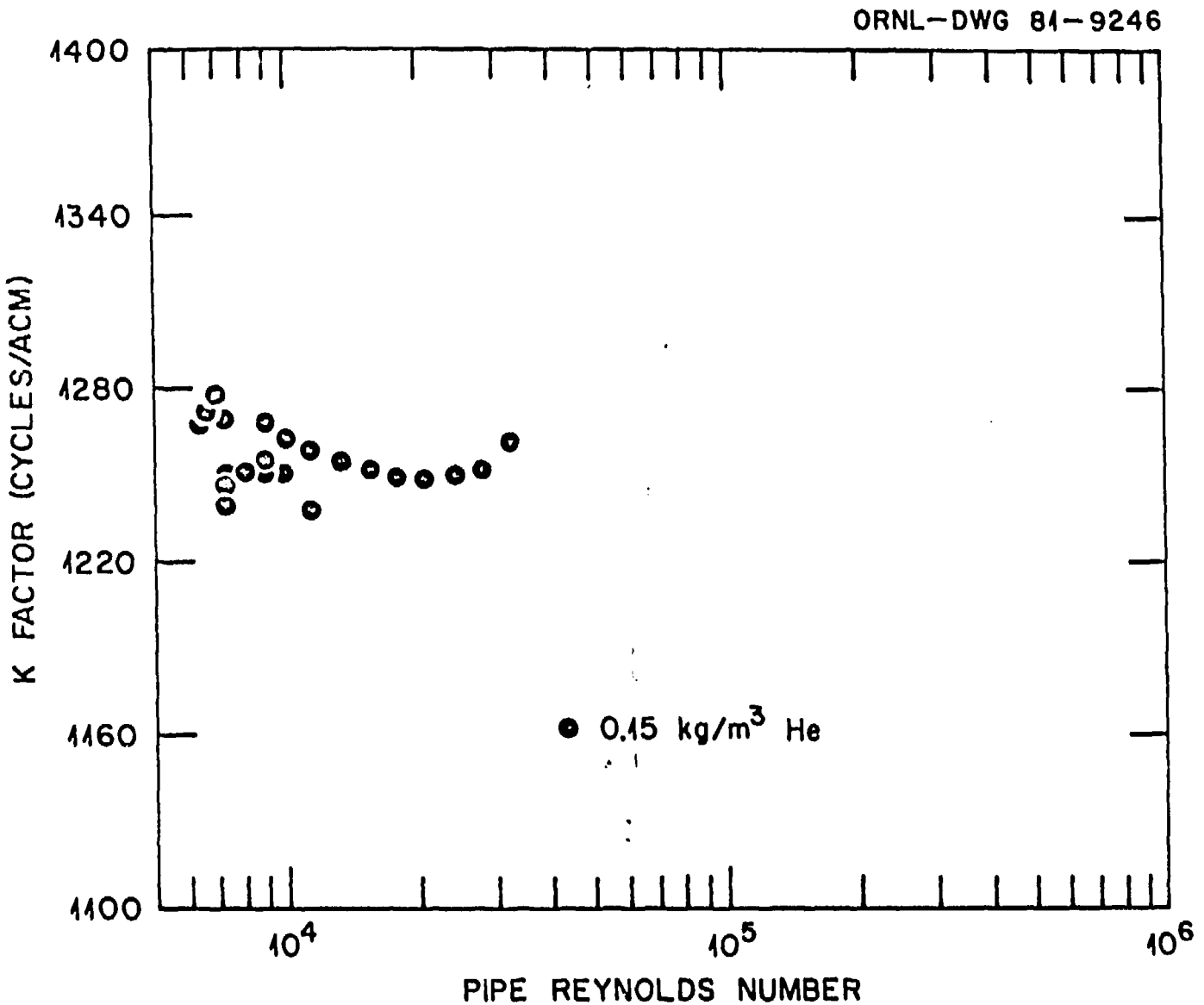

Figure 17. K factor versus Pipe Reynolds number for FE-4 (low-density helium data).

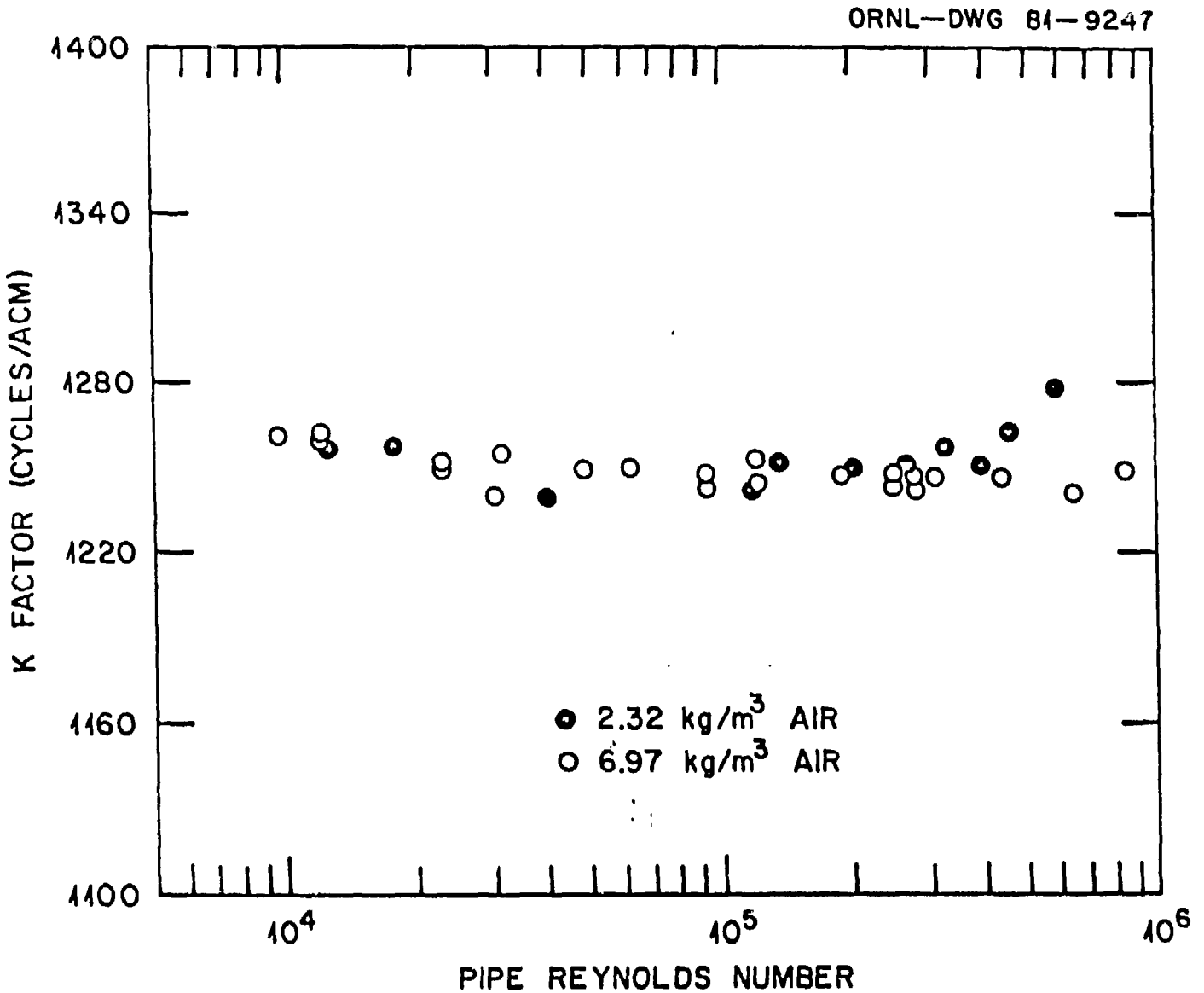

Figure 18. K factor versus Pipe Reynolds number for FE-7 (all air data).

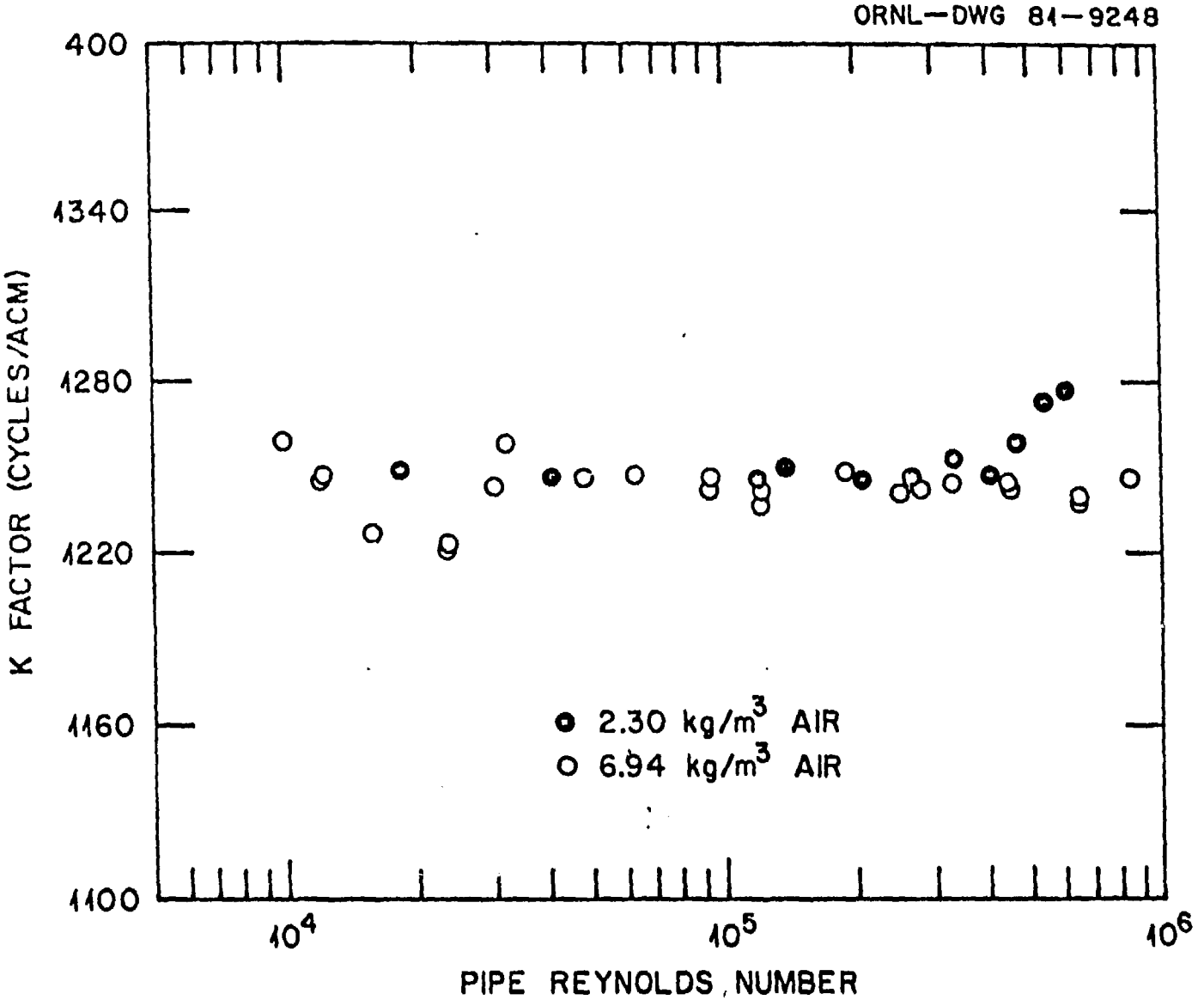

Figure 19. K factor versus Pipe Reynolds number for FE-9 (all air data).

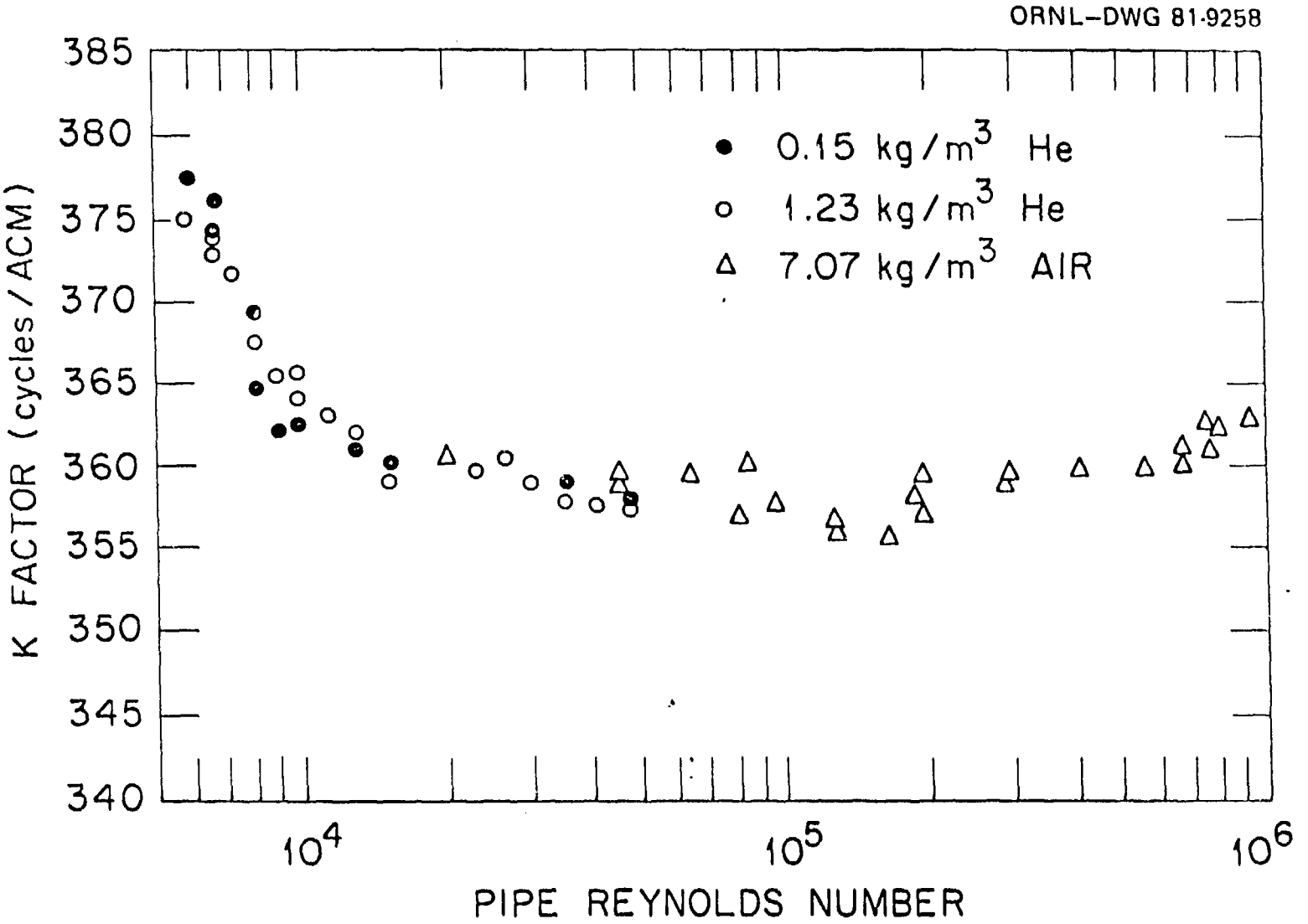

Figure 20. K Factor versus Pipe Reynolds number for FE-11 (all calibration data).

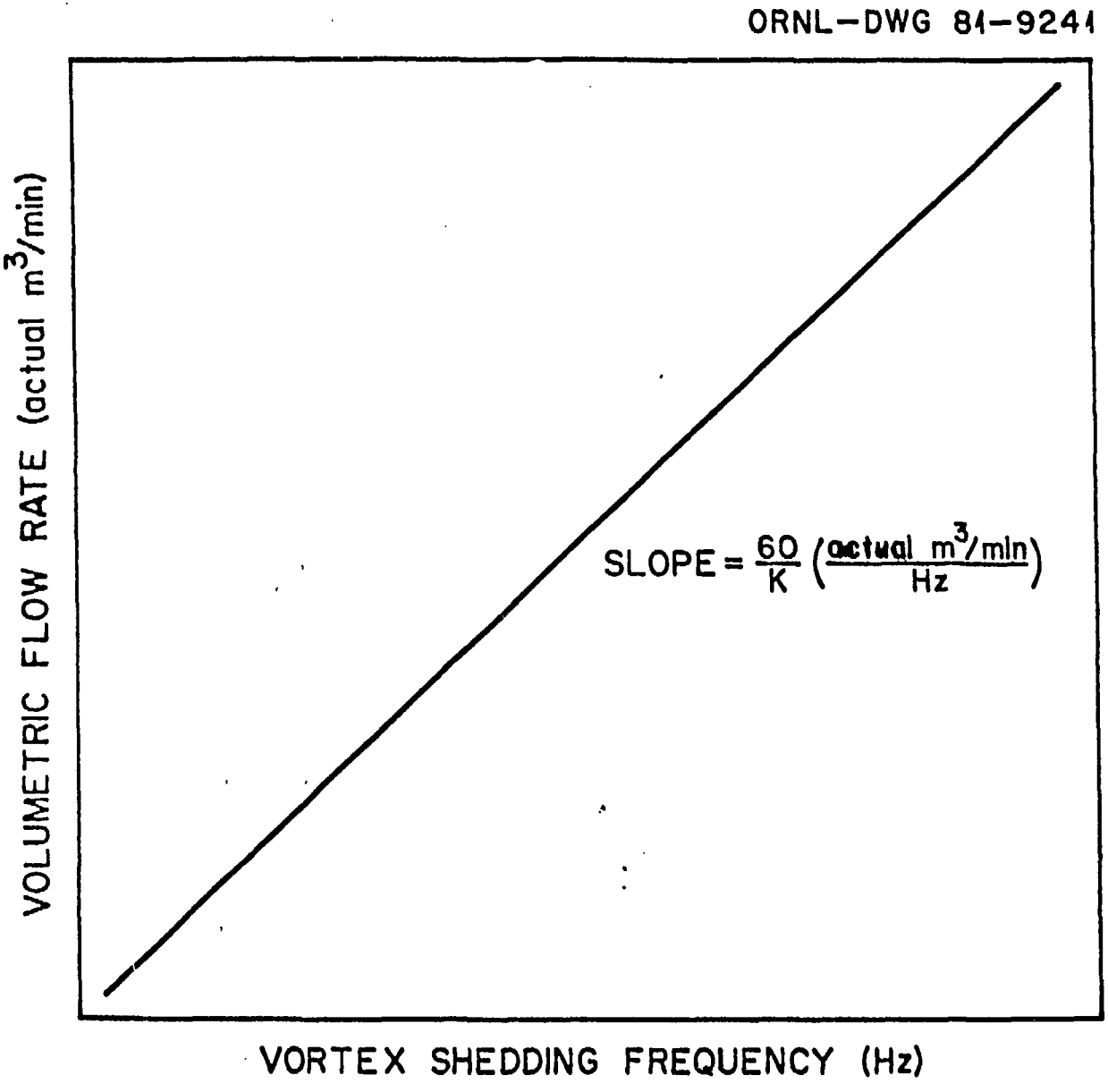

Figure A-1. General plot of volumetric flow rate versus vortex shedding frequency.